Physics Letters B 822 (2021) 136708

Contents lists available at ScienceDirect

Physics Letters B

www.elsevier.com/locate/physletb

Kaon–proton strong interaction at low relative momentum via femtoscopy in Pb–Pb collisions at the LHC

ALICE Collaboration *

ARTICLE INFO

Article history:
Received 29 July 2021
Received in revised form 29 September 2021
Accepted 1 October 2021
Available online 6 October 2021
Editor: M. Pierini

ABSTRACT

In quantum scattering processes between two particles, aspects characterizing the strong and Coulomb forces can be observed in kinematic distributions of the particle pairs. The sensitivity to the interaction potential reaches a maximum at low relative momentum and vanishing distance between the two particles. Ultrarelativistic heavy-ion collisions at the LHC provide an abundant source of many hadron species and can be employed as a measurement method of scattering parameters that is complementary to scattering experiments. This study confirms that momentum correlations of particles produced in Pb–Pb collisions at the LHC provide an accurate measurement of kaon–proton scattering parameters at low relative momentum, allowing precise access to the $\mathrm{K^-p} \rightarrow \mathrm{K^-p}$ process. This work also validates the femtoscopic measurement in ultrarelativistic heavy-ion collisions as an alternative to scattering experiments and a complementary tool to the study of exotic atoms with comparable precision. In this work, the first femtoscopic measurement of momentum correlations of $\mathrm{K^-p}$ ($\mathrm{K^+\overline{p}}$) and $\mathrm{K^+p}$ ($\mathrm{K^-\overline{p}}$) pairs in Pb–Pb collisions at centre-of-mass energy per nucleon pair of $\sqrt{s_{\mathrm{NN}}} = 5.02$ TeV registered by the ALICE experiment is reported. The components of the $\mathrm{K^-p}$ complex scattering length are extracted and found to be $\Re f_0 = -0.91 \pm 0.03(\mathrm{stat})^{+0.17}_{-0.03}(\mathrm{syst})$ and $\Im f_0 = 0.92 \pm 0.05(\mathrm{stat})^{+0.12}_{-0.33}(\mathrm{syst})$. The results are compared with chiral effective field theory predictions as well as with existing data from dedicated scattering and exotic kaonic atom experiments.

1. Introduction

The study of kaon–nucleon (KN) and antikaon–nucleon ($\overline{\mathrm{K}}$N) interactions is essential to understand low-energy quantum chromodynamics (QCD). The Goldstone boson nature of the kaon and its role as an active degree of freedom within effective field theories are used to describe processes within the chiral SU(3) dynamics at low energies. Since perturbation theory is not applicable in this energy regime, experimental data are essential to constrain the currently available effective theories [1]. In general, three experimental techniques can be used to access hadron–hadron interaction, such as $\overline{\mathrm{K}}$N, which will be discussed below. Their schematic illustration is shown in Fig. 1.

A direct measurement of the $\overline{\mathrm{K}}$N interaction was first possible in scattering experiments with secondary $\mathrm{K^-}$ beams impinging on hydrogen targets. Such experiments allow the precise control of both the initial (incoming) and final (outgoing) states, see Fig. 1 a. Furthermore, polarised beams and targets can be used [2]. However, scattering measurements can only be performed for pairs of charged and long-lived particles, because of the technical challenges of creating beams of other particle species, especially involving strangeness or antimatter [3]. Finally, attaining zero relative momentum for strange hadrons, such as kaons, is also challenging. Current $\mathrm{K^-p}$ measurements can only reach a kaon momentum of approximately 100 MeV/c with respect to the proton at rest [4–10]. Therefore, the present accuracy of the $\mathrm{K^-p}$ cross sections and branching ratios at threshold does not sufficiently constrain the scattering amplitudes.

Another way of studying the low-energy $\overline{\mathrm{K}}$N interaction is by observing the shifts and widths of energy levels in exotic kaonic atoms [11], where a negative kaon replaces an electron, see Fig. 1 b. In particular, kaonic hydrogen and kaonic deuterium can be formed in dedicated experimental setups and measurements of their X-ray deexcitation spectra provide a link to the $\mathrm{K^-p}$ strong interaction at zero relative momentum [12]. When the negative hadron, such as $\mathrm{K^-}$, transits between the lowest energy states, its wave function overlaps with the nucleus and the presence of the strong force modifies the energy levels and their widths due to coupling to intermediate states before absorption [13,14]. The measurement of the energy shift and width of the 1S state of the kaonic hydrogen line can be connected to the $\mathrm{K^-p}$ scattering length (f_0) through the Trueman–Deser formula [15,16]. How-

* *E-mail address:* alice-publications@cern.ch.

https://doi.org/10.1016/j.physletb.2021.136708

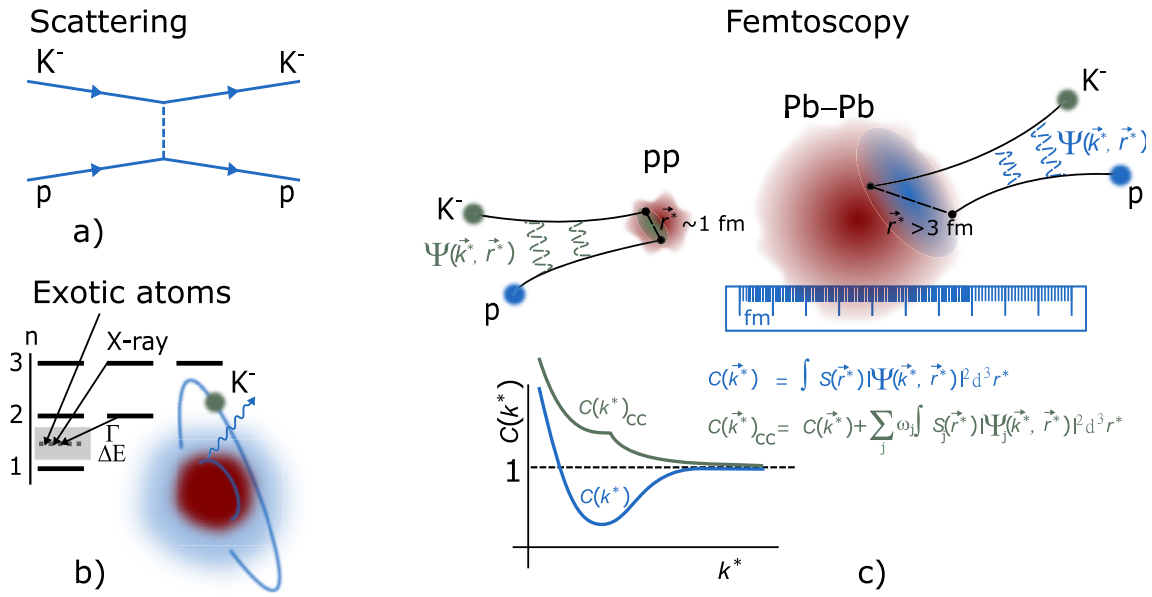

Fig. 1. Schematic illustration of available experimental techniques for measuring the interaction among hadrons: a) scattering experiments, b) measurements of energy shifts from the X-ray de-excitation spectrum of exotic atoms, c) femtoscopy in small collision systems (pp) with coupled channel effects shown in green, and in large collision systems (Pb–Pb) with vanishing coupled channel contributions shown in blue.

ever, it requires model-dependent corrections to account for the presence of the isospin-breaking couplings and the Coulomb interaction [16]. The scattering length is a complex number related to both the elastic and inelastic cross sections of the interaction. The current benchmark result is from chiral effective field theory (χ^{EFT} calculations) [17,18] anchored to the kaonic hydrogen data [19,20] collected by the SIDDHARTA experiment [21] at the DAΦNE electron–positron collider [22], and estimates the real part $\Re f_0 = -0.65 \pm 0.10$ fm[1] and the imaginary part $\Im f_0 = 0.81 \pm 0.15$ fm of the scattering length. Historically, the scattering parameters extracted from the kaonic hydrogen experiments pointed to an attractive interaction, while a repulsive $\mathrm{K^-p}$ scattering length in free space was measured via scattering experiments. Currently, both results are explained simultaneously by the presence of the $\Lambda(1405)$ resonance located just below the $\overline{\mathrm{K}}\mathrm{N}$ threshold [23]. Similar experiments have been performed with other hadrons, such as pions [14,24] and antiprotons [25], providing precise measurements of the interaction at the kinematic threshold.

On the other hand, the repulsive nature of the $\mathrm{K^+p}$ interaction is well established. It is described by an s-wave [26] scattering length with a negative real part ($\Re f_0 = -0.308 \pm 0.003$) and the Coulomb interaction [27,28].

Scattering experiments are special in that both the initial and final states are fixed, which implies that only the $\mathrm{K^-p \to K^-p}$ process can be accessed. This is not the case for ultrarelativistic particle collisions since only the $\mathrm{K^-p}$ final state is fixed and different initial states are allowed, such as $\overline{\mathrm{K}}^0\mathrm{n}$ and $\pi\Sigma$, which are referred to as coupled channels. Collisions of nuclei at the Large Hadron Collider (LHC) provide an abundant source of various particle species (including strange hadrons [29]), in both small (pp, p–Pb) and large (Pb–Pb) systems. In a single central Pb–Pb collision, the number of produced particles reaches thousands at midrapidity ($|y| < 0.5$) [30–32]. Moreover, since the baryon chemical potential for ultrarelativistic heavy-ion collisions at LHC energies approaches zero, a nearly equal amount of matter and antimatter are produced [33]. Therefore, they are an ideal environment for conducting interaction studies involving both strangeness and antimatter [34–36], as shown in Fig. 1 c. A recent breakthrough in the field was achieved by analysing the kaon–proton momentum correlations [37] using the technique of femtoscopy in high-energy pp collisions at the ALICE experiment [38], showing clear evidence for the presence of coupled channels in the measured correlation function. In particular, a clear signature for the opening at the threshold of the $\overline{\mathrm{K}}^0\mathrm{n}$ isospin breaking channel is observed due to the mass difference between the pairs.

In order to reproduce the experimental data, theoretical models need to describe the Coulomb interaction, the coupled-channels effects, and the threshold energy difference among the isospin multiplets used in the calculation [39]. This can be done in a realistic $\overline{\mathrm{K}}\mathrm{N}$–$\pi\Sigma$–$\pi\Lambda$ coupled-channel potential which can be constructed starting from chiral SU(3) dynamics [18]. Alternatively, the $\overline{\mathrm{K}}\mathrm{N}$ interaction can also be characterized by the Lednický–Lyuboshitz analytical model where the s-wave scattering parameters are used to describe the measurements [40,41].

It has been recently predicted that the strength of the coupled channels is significantly reduced for source sizes larger than 3 fm, because channels other than $\mathrm{K^-p}$ have a considerable magnitude only around a distance of 1 fm [39]. It is therefore expected that for larger sources, such as those created in heavy-ion collisions, their effect on the correlation function should be significantly reduced or become asymptotically small. Therefore, the analysis of $\mathrm{K^-p}$ pairs in Pb–Pb collisions, as shown in this work for the first time, can help to disentangle the $\mathrm{K^-p \to K^-p}$ process from contributions stemming from on-shell coupled channels at the reaction threshold.

2. Experimental setup and particle selection

The ALICE apparatus [38] is designed to measure the particles produced in proton and lead (Pb) collisions at the LHC [42]. The central barrel consists of a large solenoid magnet used to generate homogeneous magnetic fields up to 0.5 T along the beam directions and a set of detectors located in the interior surrounding the beam axis. Additional detectors are located outside the central barrel in the forward beam direction. A detailed description of the performance of the ALICE detector can be found in Ref. [43].

[1] The usual femtoscopic sign convention is used, where a positive $\Re f_0$ corresponds to attractive strong interaction.

Table 1
Centrality ranges and corresponding average charged-particle multiplicity densities at midrapidity $\langle dN_{ch}/d\eta \rangle$ for Pb–Pb collisions at $\sqrt{s_{NN}} = 5.02$ TeV [45].

Centrality	$\langle dN_{ch}/d\eta \rangle$
0–5%	1943 ± 53
5–10%	1586 ± 46
10–20%	1180 ± 31
20–30%	786 ± 20
30–40%	512 ± 15
40–50%	318 ± 12

In this work, the minimum-bias Pb–Pb data at a collision energy per nucleon–nucleon pair of $\sqrt{s_{NN}} = 5.02$ TeV collected by ALICE in the LHC Run 2 (2015) are used. The recording of the collisions products was triggered using the V0 detector consisting of two arrays of 32 scintillator counters covering pseudorapidity (η) ranges of $2.8 < \eta < 5.1$ (V0A) and $-3.7 < \eta < -1.7$ (V0C). A coincident signal in both detectors consistent with the collision occurring at the centre of the ALICE detector was required. The centrality of the collision, expressed in percentages of the total hadronic cross section, was determined using the amplitudes of the signals in the V0 detectors following the procedure described in Ref. [44] and classified into six intervals of the Pb–Pb cross section: 0–5%, 5–10%, 10–20%, 20–30%, 30–40%, and 40–50%. Those intervals together with the corresponding charged-particle multiplicity densities at midrapidity $\langle dN_{ch}/d\eta \rangle$ are listed in Table 1. Only collisions within ± 10 cm of the nominal interaction point along the beam axis are considered in this analysis in order to achieve uniform tracking and particle identification performance.

For track reconstruction and hadron identification the analysis uses information provided by the Inner Tracking System (ITS) [38], the Time Projection Chamber (TPC) [38,46], and the Time-of-Flight detector (TOF) [47], located inside the solenoid magnet.

The ITS is composed of six cylindrical layers of silicon detectors and it is used to determine the locations of the primary vertex by extrapolation of primary tracks.

The TPC is a large (volume of 88 m^3) cylindrical detector filled with gas and is used as the main tracking and particle identification detector of ALICE. The central electrode divides the TPC into two halves. At the end of each half there is a readout plane composed of 18 sectors (with full azimuthal angle φ coverage). Each sector contains 159 padrows arranged radially. A track signal in the TPC consists of space points (referred to as *clusters*), each reconstructed in one of the padrows. A Kalman fit is performed on a set of clusters in order to obtain the parameters of a given track. In this analysis, the determination of momentum is performed using the track curvature from the TPC detector only.

TOF is a cylindrical detector composed of Multigap Resistive Plate Chambers (MRPC) located at $r \cong 380$ cm from the beam axis. They are also arranged into 18 azimuthal sectors. The detector measures the arrival of particles with a precision of the order of 50 ps.

Acceptance is restricted to $|\eta| < 0.8$. Selected kaons have transverse momenta of $0.19 < p_T < 0.45$ GeV/c, while for protons the interval is $0.5 < p_T < 4.0$ GeV/c. The distances of closest approach (DCA) of a proton track to the primary vertex in the transverse (DCA_{XY}) and longitudinal (DCA_Z) directions are required to be less than $0.0105 + 0.0350/(p_T/(\text{GeV}/c)^{-1.1})$ cm and 3.2 cm, respectively. These selections are imposed to reduce the contamination from secondary tracks originating from weak decays and from interaction with the detector material. All selections are summarized in Table 2.

Particle identification is based on energy loss dE/dx in the TPC and time of flight in the TOF. The difference between the measured and expected signals can be expressed in units of detector resolution called N_σ. For protons, the combined signal from TOF and TPC is allowed to differ from the expected one by $N_\sigma = 3\sqrt{2}$. For kaons, five selection criteria (depending on the momentum p) were introduced, as detailed in Table 2. The selection criteria are optimised to obtain a high-purity sample without compromising the efficiency. The identification purity of the data sample is estimated from detailed Monte Carlo (MC) simulations using the HIJING [48] event generator coupled to the GEANT3 [49] transport package and found to be above 98.5% for both the kaon and proton samples. The fraction of protons originating from weak decays is determined to be 5.6% and negligible for kaons ($< 0.05\%$). An additional method based on template fits to the distributions of the DCA_Z is used to determine the contribution from weak decays in the proton sample. The fraction of 7.9% obtained for secondary protons is averaged with the fraction from MC, resulting in a contamination of 6.5% of weak decays in the sample.

Table 2
Single particle selection criteria for kaons and protons.

Track selection	
$K^{\pm}$ p_T	$0.19 < p_T < 0.45$ GeV/c
$p/\bar{p}$ p_T	$0.5 < p_T < 4$ GeV/c
$\lvert\eta\rvert$	< 0.8
DCA_z to primary vertex	< 3.2 cm
Kaon selection	
$N_{\sigma,TPC}$ (for $p < 0.4$ GeV/c)	< 2
$N_{\sigma,TPC}$ (for $0.4 < p < 0.45$ GeV/c)	< 1
$N_{\sigma,TPC}$ (for $p > 0.45$ GeV/c)	< 3
$N_{\sigma,TOF}$ (for $0.5 < p < 0.8$ GeV/c)	< 2
$N_{\sigma,TOF}$ (for $0.8 < p < 1.0$ GeV/c)	< 1.5
$N_{\sigma,TOF}$ (for $1.0 < p < 1.5$ GeV/c)	< 1
DCA_{xy} to primary vertex	2.4 cm
Proton selection	
$\sqrt{N^2_{\sigma,TPC} + N^2_{\sigma,TOF}}$ (for $p_T > 0.5$ GeV/c)	$< 3\sqrt{2}$
DCA_{xy} to primary vertex	$0.0105 + 0.0350/(p_T/(\text{GeV}/c)^{-1.1})$ cm

The identified tracks from each event are combined into pairs to form the distribution $A(k^*)$. Two-particle detector acceptance effects, including track splitting, track merging, as well as effects coming from $\gamma \to e^+e^-$ conversion, contribute to the measured distributions. The following selections are applied to reduce these effects. For pairs of tracks within the relative pseudorapidity of the two tracks $|\Delta\eta| < 0.01$, an exclusion on the fraction of merged points is introduced. The merged fraction is defined as the ratio of the number of steps of 1 cm considered in the TPC radius range for which the distance between the tracks is less than 3 cm, to the total number of steps. Pairs with a merged fraction above 3% are removed. The e^+e^- pairs originating from photon conversions can be misidentified as real kaon–proton pairs and it is necessary to remove spurious correlations arising from such pairs. These pairs are removed if their invariant mass, assuming the electron mass for both particles, is less than 0.002 GeV/c^2, and the relative polar angle, $\Delta\theta$, between the two tracks is less than 0.008 rad.

3. Data analysis

The femtoscopic measurements are based on the sensitivity of two-particle correlations at low relative momentum to the space–time separation of the particle emitters due to the effects of quantum statistics and/or final state interactions (FSI), i.e. Coulomb and strong forces, depending on the pair under consideration [50,51]. The femtoscopic correlation function, as shown in Fig. 1 c, in the pair rest frame (PRF) can be written as [52,53]

$$C(\vec{k}^*) = \int S(\vec{r}^*) \left|\Psi(\vec{k}^*, \vec{r}^*)\right|^2 d^3r^*, \quad (1)$$

Table 3
Components of the systematic uncertainty expressed as relative uncertainties from various sources. For a detailed description of each variation see the text.

Variation	ΔR_{Kp} (%)						$\Delta\Re f_0$ (%)	$\Delta\Im f_0$ (%)
	Centrality							
	0–5%	5–10%	10–20%	20–30%	30–40%	40–50%		
Background 1	4	<1	<1	<1	<1	<1	3	1
Background 2	3	3	4	3	1	3	6	13
Pair purity −3%	−3	−4	−3	−3	−3	−3	+1	−5
Pair purity +3%	+6	+4	+7	+4	+4	+4	−2	+11
Momentum resolution	−14	−13	−9	−11	−10	−10	+19	−27
Fit range 0–0.2 GeV/c	5	2	1	1	<1	<1	2	<1
Fit range 0.005–0.150 GeV/c	3	3	8	<1	<1	<1	4	1
Alternative DCA selection	8	6	4	6	<1	7	1	5
Kaon selection (low and high p_{T})	−11	−8	−8	−13	−5	−4	+16	−10
Kaon selection (high p_{T} only)	Does not apply						+19	−35

where $|\vec{k}^*| = k^*$ is half the kaon–proton pair relative momentum, which is equal to the momentum of the first particle in the PRF, where the pair centre of mass is at rest ($\vec{p}_1 = -\vec{p}_2$). The two-particle emitting source function is denoted as $S(\vec{r}^*)$, $\Psi(\vec{k}^*, \vec{r}^*)$ is the pair wave function, and $\vec{r}^*$ is the relative separation vector. The pair wave function depends on the interactions between the two hadrons [40,41]. In the case of equal emission time in the PRF, the Bethe–Salpeter amplitude in the Lednický–Lyuboshitz formalism [40,41,54], described in detail in Appendix A, coincides with a stationary solution of the scattering problem with reversed time direction in the emission process. The interaction then depends only on the scattering length, f_0, and the effective range of the interaction, d_0. In this work, the spin-averaged scattering parameters are obtained, i.e. the real and imaginary parts, $\Re f_0$ and $\Im f_0$, respectively, of the scattering length. Moreover, the zero-effective-range approximation ($d_0 = 0$) is used in the analysis.

The experimental correlation function, $C(k^*) = \mathcal{N}\ A(k^*)/B(k^*)$, is constructed as a ratio between the measured distribution of pair relative momenta $A(k^*)$ and the uncorrelated distribution $B(k^*)$ obtained using the mixed-event technique [55,56], where $\mathcal{N}$ is a free normalization factor which is constrained by $C(k^*) = 1$ at $300 < k^* < 800$ MeV/c. Effects of the scattering length as well as of the size of the femtoscopic source are studied in the region of $k^* < 150$ MeV/c. Deviations from unity of $C(k^*)$ in this region indicate the presence of an interaction between the studied particles. In general, the attractive or repulsive forces manifest themselves in values of the correlation function greater or smaller than one, respectively [57].

The femtoscopic correlation functions for $\mathrm{K}^-\mathrm{p}$ and $\mathrm{K}^+\mathrm{p}$ pairs and their charge conjugates $\mathrm{K}^+\overline{\mathrm{p}}$ and $\mathrm{K}^-\overline{\mathrm{p}}$ are measured in six centrality intervals [44]. The centrality intervals and the corresponding charged-particle multiplicity densities at midrapidity $\langle \mathrm{d}N_{\mathrm{ch}}/\mathrm{d}\eta \rangle$ are listed in Table 1. Since no deviations, apart from statistical ones, between pairs and corresponding charge conjugate pairs are observed, they are combined and denoted as $\mathrm{K}^+\mathrm{p} \oplus \mathrm{K}^-\overline{\mathrm{p}}$ for same- and $\mathrm{K}^-\mathrm{p} \oplus \mathrm{K}^+\overline{\mathrm{p}}$ for opposite-charge combinations, respectively.

In Pb–Pb collisions, particles are also correlated due to the collective expansion of the system. This generates a slope in the correlation function [58] which appears to be well described by both hydrodynamic simulations [59] coupled to the statistical hadronisation code THERMINATOR 2 [60] or using the AMPT model [61]. These background correlations are therefore subtracted before fitting the correlation functions by employing a first-order polynomial fit to the AMPT simulated data in the first two centrality intervals (0–10%) and a fit to the THERMINATOR 2 simulated data for the remaining centrality classes (10–50%). The fixed value of the impact parameter used for 0–10% centrality interval in THERMINATOR 2 was not reproducing the distribution of measured average charged-particle multiplicity.

The extraction of the scattering length parameters of $\mathrm{K}^-\mathrm{p} \oplus \mathrm{K}^+\overline{\mathrm{p}}$ pairs from the measured correlation functions uses a dedicated fitting procedure based on the Lednický–Lyuboshitz formalism. A simultaneous fit to all measured pairs in the six centrality classes is performed in the range up to $k^* = 175$ MeV/c. The final values of the fitted parameters are obtained from the comparison of the experimental correlation functions to the set of precomputed model functions and based on the lowest χ^2/ndf.

The assumption for the source function $S(\vec{r}^*)$ is that, for each centrality, it is a three-dimensional spheroid with a Gaussian density profile in the PRF [56,62,63] with a common width parameter for same- and opposite-charge pairs R_{Kp}, referred to as the source size or femtoscopic radius. This assumption is based on hydrodynamic models [64,65] of the matter produced in ultrarelativistic heavy-ion collisions which provide quantitative agreement [66] with collective phenomena [67], particle transverse-momentum spectra [68], and femtoscopy of both identical [56,69] and non-identical particles [63]. The femtoscopic radii follow the previously observed linear scaling with $\langle \mathrm{d}N_{\mathrm{ch}}/\mathrm{d}\eta \rangle^{1/3}$ and the transverse-mass scaling behaviour [69–73]. This allows one to fix the source functional form in Eq. (1) and use the Lednický–Lyuboshitz formalism for measurements of the interaction between any pair of particles that can be detected in the final state. Moreover, the fit is further constrained by using the measured scattering length values for $\mathrm{K}^+\mathrm{p} \oplus \mathrm{K}^-\overline{\mathrm{p}}$ pairs, established from a partial wave analysis to be $\Re f_0 = -0.308 \pm 0.003$ fm [28]. Finally, there are six different femtoscopic radii corresponding to each centrality class and two, real and imaginary, components of the $\mathrm{K}^-\mathrm{p} \oplus \mathrm{K}^+\overline{\mathrm{p}}$ scattering length. In a simultaneous fit to all measured correlation functions, the fitting procedure determines the six radii from the $\mathrm{K}^+\mathrm{p}$ correlations and the real and imaginary parameters of the strong interaction scattering length from the $\mathrm{K}^-\mathrm{p}$ correlations.

The fitting procedure also accounts for the purity of the sample, defined as the percentage of properly identified primary particle pairs originating from the three-dimensional Gaussian profile of the source, following the method described in Ref. [74]. This method was successfully employed in the pion–kaon femtoscopic analysis by ALICE [63]. The value for the purity parameter was estimated to be 87% and depends on the misidentification, secondary contamination from weak decays, and percentage of kaons and protons that come from strongly decaying resonances constituting the long tails in the source distribution, outside the Gaussian core.

The measured correlation function is also affected by the finite momentum resolution of the ALICE detector. The detector response matrix is obtained using a detailed Monte Carlo simulation of the detector based on HIJING [48] coupled to GEANT3 [49] transport code and is used to smear the theoretical calculations.

4. Systematic uncertainties

The final systematic uncertainties are the maximum and minimum deviations from the reference values obtained for different variations of the analysis. The relative values of the important sources of uncorrelated systematic uncertainty are listed in Table 3. One of the most significant sources of uncertainty comes from background estimation. The analysis considers two variations of the default option. The first one (Background 1) defines the background as a first-order polynomial fit to the raw data in the k^* region 0.35–0.6 GeV/c instead of predictions from the AMPT model in the first two centrality intervals. The second one (Background 2) estimates the background from the average of the first-order polynomial fit to the raw data and the AMPT prediction in the first two centrality intervals and the average of functions provided by the THERMINATOR 2 code and the AMPT model in the other four centrality intervals. The pair purity value used for scaling data points is also varied. The default value equals 87%, the effect of possible additional sources of impurities is evaluated and found to be smaller than 7%. The systematic effect of the finite resolution of the detectors is evaluated using an alternative technique based on a smoothed detector response matrix. Another variation of the default analysis is obtained by using a different sample of kaons. The default data contain kaons in the transverse-momentum range between 0.19–0.45 GeV/c, while the variations cover the regions of 0.5–1.5 GeV/c as well as 0.19–1.5 GeV/c. The sample with high p_{T} is the most significant source of the uncertainty of the real and imaginary parts of the scattering length due to the change in the average pair transverse mass m_{T} (the changes of radii are expected and should not be treated as systematic uncertainty). The systematic uncertainty related to the DCA is evaluated using an alternative selection of a p_{T} dependent $\mathrm{DCA_Z} < 0.418 - 0.372 \times p_{\mathrm{T}}^{0.66}$ cm and a constant value of $\mathrm{DCA_{XY}} < 2.4$ cm, preserving the integrated proton purity. Additionally, results from the combined fit to both kaon selections are also taken into account where the high p_{T} kaon sample radii are scaled to the low-p_{T} according to the average pair m_{T}. Variations of the fitting range and track reconstruction have a negligible contribution compared with other sources.

5. Results

The correlation functions for opposite-charge particle pairs ($\mathrm{K^-p} \oplus \mathrm{K^+\overline{p}}$), after division by the AMPT or THERMINATOR 2 baselines, are shown in Fig. 2. The correlation functions for same-charge particle pairs ($\mathrm{K^+p} \oplus \mathrm{K^-\overline{p}}$) are presented as inserts. The cyan band represents the result of the simultaneous fit to all obtained correlation functions with the Lednický–Lyuboshitz model [40,41]. The orange band corresponds to predictions from χ^{EFT} calculations. These are computed using the Kyoto model [39] and evaluated with the CATS framework [80]. The Kyoto model is based on a chiral effective SU(3) calculation in which all coupled channels, such as $\mathrm{\overline{K}^0n}$ and $\pi\Sigma$ are included. At present, this model is able to describe both the ALICE results from proton–proton collisions [37] and the SIDDHARTA measurement [18]. The bottom panels of Fig. 2 show the difference between the data and the fit (model) divided by the statistical uncertainty of the data, σ_{stat}.

The following effects can be observed: the $\mathrm{K^-p} \oplus \mathrm{K^+\overline{p}}$ pairs show an attractive Coulomb interaction for small k^*. The effect is opposite for $\mathrm{K^+p} \oplus \mathrm{K^-\overline{p}}$ pairs. The influence of the repulsive strong interaction manifests as correlation functions reaching values below unity in the region of $k^* \approx 20 - 50$ MeV/c and becomes more pronounced towards more peripheral events, i.e., smaller source sizes. As predicted in Ref. [39], features of the correlation function related to the coupled channels, observed in the analysis of pp collisions [37], are negligible here. Neither the cusp structure at 58 MeV/c due to the presence of the isospin-breaking channel $\mathrm{K^0n} \rightarrow \mathrm{K^-p}$ nor the enhancement due to the coupled channels below threshold enhancing the correlation above unity in the intermediate k^* range are visible in the correlation function in Pb–Pb.

The common femtoscopic radii R_{Kp} for same- and opposite-charge pairs obtained from the Lednický–Lyuboshitz fit are provided in Fig. 2 as well. They increase from around 5 fm for peripheral events to almost 9 fm for central events, and all are larger than 3 fm where the predicted effect of coupled channels is reduced or negligible [39]. The radii scale linearly with the cube root of the mean charged-particle multiplicity density $\langle \mathrm{d}N_{\mathrm{ch}}/\mathrm{d}\eta \rangle^{1/3}$, as observed for pion–pion [73], kaon–kaon [56], and pion–kaon [63] pairs. The scattering length parameters obtained from the fit are $\Re f_0 = -0.91 \pm 0.03(\mathrm{stat})^{+0.17}_{-0.03}(\mathrm{syst})$ fm and $\Im f_0 = 0.92 \pm 0.05(\mathrm{stat})^{+0.12}_{-0.33}(\mathrm{syst})$ fm.

The obtained parameters of the scattering length are compared with the available experimental values as well as model calculations [18,75–79] in the left panel of Fig. 3. Numerical values of those parameters are also provided in Table 4. The ALICE results are compatible with them within uncertainties.[2] Up until this point, the world's best experimental data on Kp scattering are mainly from exotic kaonic atoms, where the interaction at the threshold is measured, and from scattering experiments. Theory predictions and calculations are based on χ^{EFT} models.

Moreover, the Lednický–Lyuboshitz formalism is also used to compute femtoscopic correlation functions using scattering length parameters from previous measurements and theory predictions. They are then compared with the experimental data and the deviations in units of χ^2/ndf are obtained. The result of such a procedure is shown in Fig. 3 (right), while the χ^2/ndf values are presented in Table 4. The Kyoto model, which captures well the structures related to coupled channels in pp collisions, reproduces the data trends in all measured Pb–Pb centrality intervals, confirming that the coupled channels are fundamental in the description of small sources but have a negligible influence on correlation functions at large source sizes [39]. However, the model still requires further development as the resulting $\chi^2/\mathrm{ndf} = 2.8$ is slightly worse than the best calculations using the Lednický–Lyuboshitz analytical approach.

6. Summary

In this work, we present the first measurement of non-identical particle femtoscopy of $\mathrm{K^-p} \oplus \mathrm{K^+\overline{p}}$ and $\mathrm{K^+p} \oplus \mathrm{K^-\overline{p}}$ pairs performed in Pb–Pb collisions at $\sqrt{s_{\mathrm{NN}}} = 5.02$ TeV in six centrality intervals. Up to now, the existing experimental data on $\mathrm{K^-p}$ scattering allowed us to study the interaction at a fixed range, either in the asymptotic regime, where the effect of the coupled channels is not present, or at very small ranges ($R_{\mathrm{Kp}} \sim 1$ fm) where they are dominant and difficult to disentangle from the $\mathrm{K^-p} \rightarrow \mathrm{K^-p}$ channel. The analysis of the Pb–Pb data with the ALICE detector addresses these issues by testing the $\mathrm{K^-p}$ interaction as a function of the source size in the range $R_{\mathrm{Kp}} \in (4.9, 8.9)$ fm. In femtoscopy, a precise knowledge of the source from which hadrons are emitted is needed to measure the interaction using quantum scattering theory. In the case of pp collisions, where this is of the order of 1 fm, very short interaction distances are probed. In Pb–Pb collisions, the larger average distance of several fm between the hadrons probes the asymptotic form of the two-particle wave function, as demonstrated in this work. The obtained values of R_{Kp} follow a linear scaling with the cube root of averaged charged-particle multiplicity density and the transverse-mass scaling. This is in

[2] Note that systematic uncertainties are not provided for some of the older results.

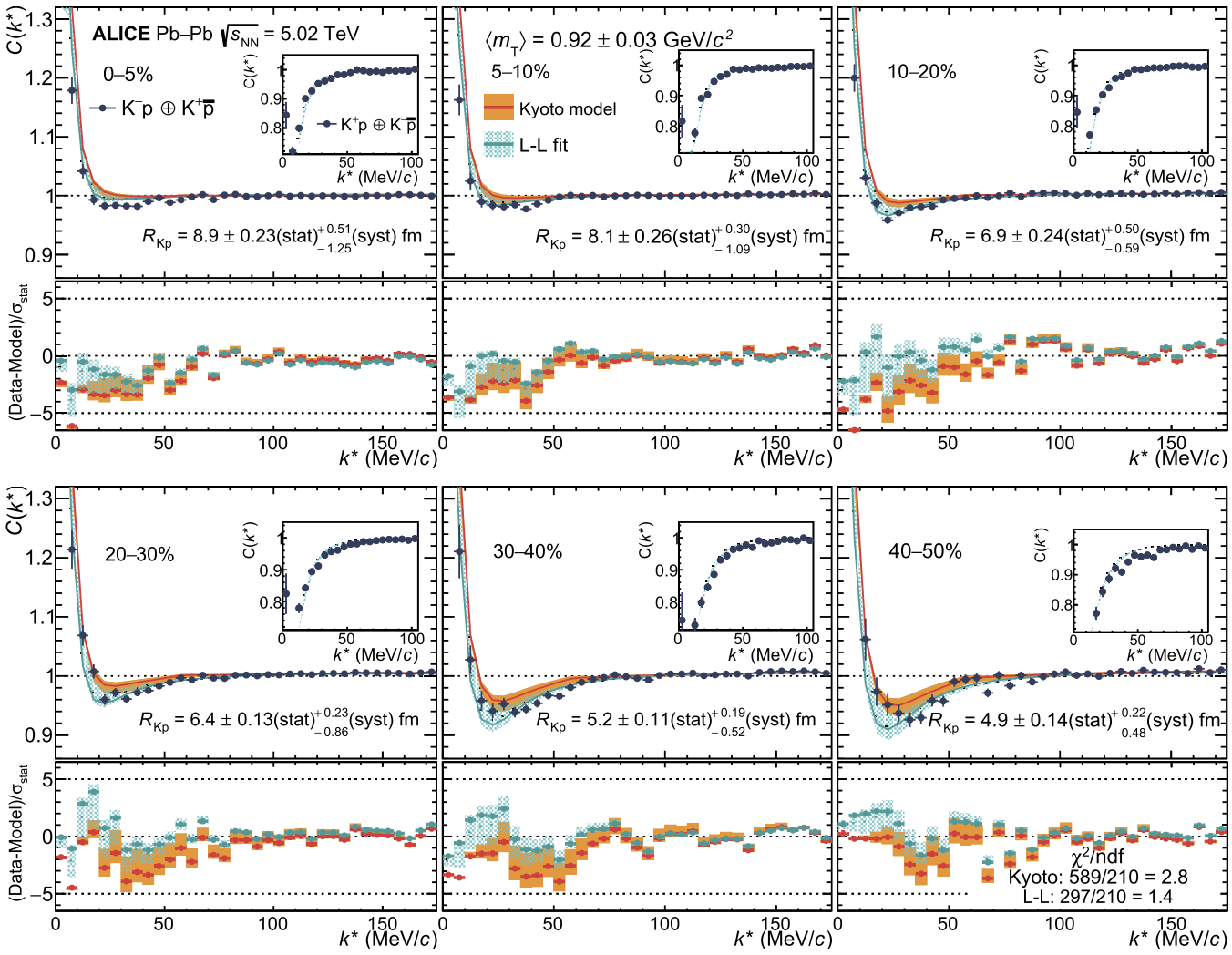

Fig. 2. The $K^-p \oplus K^+\overline{p}$ correlation functions in the six centrality classes, with the corresponding Lednický–Lyuboshitz fits (denoted as "L–L") and Kyoto model calculations shown as light cyan and orange bands, respectively. The width of the bands corresponds to the 1-σ uncertainties. The inserts show the $K^+p \oplus K^-\overline{p}$ correlation functions with Lednický–Lyuboshitz fits as light cyan bands. The bottom panels show the difference between data and the fit (model) normalised by the statistical uncertainty of the data σ_{stat}. The average pair transverse mass $\langle m_T \rangle$ is 0.92 ± 0.03 GeV/c^2 for all centrality intervals. The statistical and systematic uncertainties are added in quadrature and shown as vertical bars.

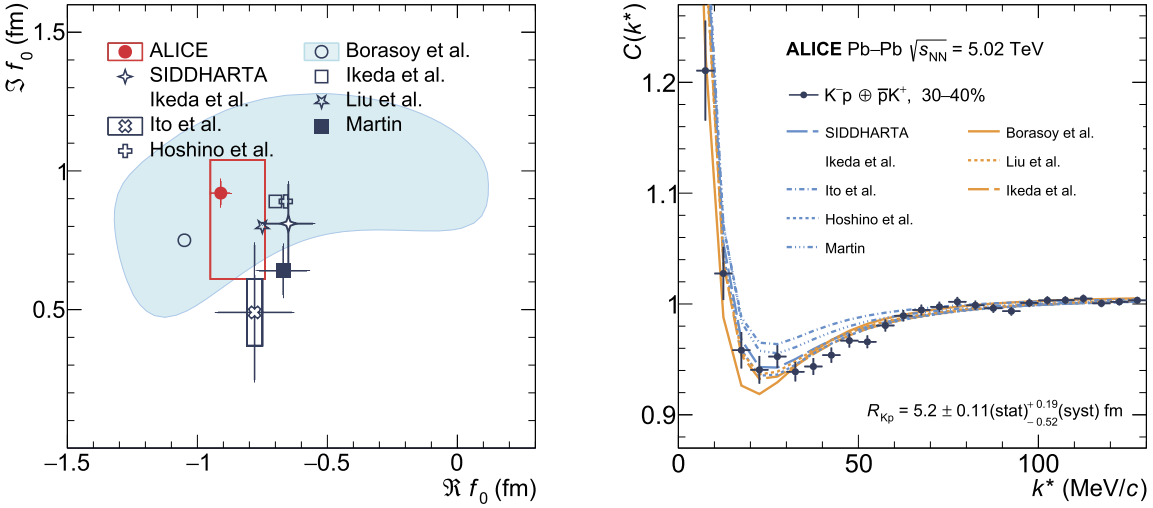

Fig. 3. Left: scattering parameters obtained from the Lednický–Lyuboshitz fit compared with available world data and theoretical calculations. Statistical uncertainties are represented as bars and systematic uncertainties, if provided, as boxes. Right: experimental femtoscopic correlation function for $K^-p \oplus K^+\overline{p}$ pairs in the 30–40% centrality interval, together with various Lednický–Lyuboshitz calculations obtained using the scattering length parameters from Refs. [17,18,75–79] and the source radius from this analysis. The statistical and systematic uncertainties of the measured data points are added in quadrature and shown as vertical bars.

Table 4
Values of the scattering parameters and the χ^2/ndf for the deviation between the ALICE data and available model calculations and previous measurements for K^-p pairs at low relative momentum.

Model calculation:	$\Re f_0$ (fm)	$\Im f_0$ (fm)	χ^2/ndf
Lednický–Lyuboshitz fit to data	$-0.91\pm 0.03(\text{stat})^{+0.17}_{-0.03}(\text{syst})$	$0.92\pm 0.05(\text{stat})^{+0.12}_{-0.33}(\text{syst})$	1.4
Kyoto [39,80]	–	–	2.8
Lednický–Lyuboshitz with fixed parameters from:			
Kaonic deuterium (Hoshino et al.) [78]	−0.66	0.89	2.0
Scattering experiments (Martin) [75]	−0.67±0.1	0.64±0.1	3.3
Chiral SU(3) (Ikeda et al.) [17,18]	−0.7	0.89	1.9
SIDDHARTA chiral SU(3) [17,18]	−0.65±0.1	0.81±0.15	2.3
Hamiltonian EFT (Liu et al.) [77]	−0.75	0.80	1.9
Kaonic hydrogen (Ito et al.) [76]	−0.78±0.15	0.49±0.25	4.2
Chiral SU(3) (Borasoy et al.) [79]	−1.05±0.5	0.75±0.4	1.6

agreement with other femtoscopic measurements in heavy-ion collisions, as expected from the hydrodynamic models. The resulting correlation functions are fitted simultaneously to extract the complex scattering length whose components are $\Re f_0 = -0.91 \pm 0.03(\text{stat})^{+0.17}_{-0.03}(\text{syst})$ fm and $\Im f_0 = 0.92 \pm 0.05(\text{stat})^{+0.12}_{-0.33}(\text{syst})$ fm. The obtained result is consistent with existing data from scattering experiments. Moreover, theoretical computations based on χ^{EFT} (the Kyoto model) provide a comparably good description across all centrality intervals, providing further confirmation on the validity of the model.

Declaration of competing interest

The authors declare that they have no known competing financial interests or personal relationships that could have appeared to influence the work reported in this paper.

Acknowledgements

The ALICE Collaboration would like to thank all its engineers and technicians for their invaluable contributions to the construction of the experiment and the CERN accelerator teams for the outstanding performance of the LHC complex. The ALICE Collaboration gratefully acknowledges the resources and support provided by all Grid centres and the Worldwide LHC Computing Grid (WLCG) collaboration. The ALICE Collaboration acknowledges the following funding agencies for their support in building and running the ALICE detector: A. I. Alikhanyan National Science Laboratory (Yerevan Physics Institute) Foundation (ANSL), State Committee of Science and World Federation of Scientists (WFS), Armenia; Austrian Academy of Sciences, Austrian Science Fund (FWF): [M 2467-N36] and Nationalstiftung für Forschung, Technologie und Entwicklung, Austria; Ministry of Communications and High Technologies, National Nuclear Research Center, Azerbaijan; Conselho Nacional de Desenvolvimento Científico e Tecnológico (CNPq), Financiadora de Estudos e Projetos (Finep), Fundação de Amparo à Pesquisa do Estado de São Paulo (FAPESP) and Universidade Federal do Rio Grande do Sul (UFRGS), Brazil; Ministry of Education of China (MOEC), Ministry of Science & Technology of China (MSTC) and National Natural Science Foundation of China (NSFC), China; Ministry of Science and Education and Croatian Science Foundation, Croatia; Centro de Aplicaciones Tecnológicas y Desarrollo Nuclear (CEADEN), Cubaenergía, Cuba; The Ministry of Education, Youth and Sports of the Czech Republic, Czech Republic; The Danish Council for Independent Research | Natural Sciences, the Villum Fonden and Danish National Research Foundation (DNRF), Denmark; Helsinki Institute of Physics (HIP), Finland; Commissariat à l'Énergie Atomique (CEA) and Institut National de Physique Nucléaire et de Physique des Particules (IN2P3) and Centre National de la Recherche Scientifique (CNRS), France; Bundesministerium für Bildung und Forschung (BMBF) and GSI Helmholtzzentrum für Schwerionenforschung GmbH, Germany; General Secretariat for Research and Technology, Ministry of Education, Research and Religions, Greece; National Research, Development and Innovation Office, Hungary; Department of Atomic Energy, Government of India (DAE), Department of Science and Technology, Government of India (DST), University Grants Commission, Government of India (UGC) and Council of Scientific and Industrial Research (CSIR), India; Indonesian Institute of Sciences, Indonesia; Istituto Nazionale di Fisica Nucleare (INFN), Italy; Institute for Innovative Science and Technology, Nagasaki Institute of Applied Science (IIST), Japanese Ministry of Education, Culture, Sports, Science and Technology (MEXT) and Japan Society for the Promotion of Science (JSPS) KAKENHI, Japan; Consejo Nacional de Ciencia (CONACYT) y Tecnología, through Fondo de Cooperación Internacional en Ciencia y Tecnología (FONCICYT) and Dirección General de Asuntos del Personal Academico (DGAPA), Mexico; Nederlandse Organisatie voor Wetenschappelijk Onderzoek (NWO), Netherlands; The Research Council of Norway, Norway; Commission on Science and Technology for Sustainable Development in the South (COMSATS), Pakistan; Pontificia Universidad Católica del Perú, Peru; Ministry of Education and Science, National Science Centre and WUT ID-UB, Poland; Korea Institute of Science and Technology Information and National Research Foundation of Korea (NRF), Republic of Korea; Ministry of Education and Scientific Research, Institute of Atomic Physics and Ministry of Research and Innovation and Institute of Atomic Physics, Romania; Joint Institute for Nuclear Research (JINR), Ministry of Education and Science of the Russian Federation, National Research Centre Kurchatov Institute, Russian Science Foundation and Russian Foundation for Basic Research, Russia; Ministry of Education, Science, Research and Sport of the Slovak Republic, Slovakia; National Research Foundation of South Africa, South Africa; Swedish Research Council (VR) and Knut and Alice Wallenberg Foundation (KAW), Sweden; European Organization for Nuclear Research, Switzerland; Suranaree University of Technology (SUT), National Science and Technology Development Agency (NSDTA) and Office of the Higher Education Commission under NRU project of Thailand, Thailand; Turkish Energy, Nuclear and Mineral Research Agency (TENMAK), Turkey; National Academy of Sciences of Ukraine, Ukraine; Science and Technology Facilities Council (STFC), United Kingdom; National Science Foundation of the United States of America (NSF) and United States Department of Energy, Office of Nuclear Physics (DOE NP), United States of America.

Appendix A. Lednický–Lyuboshitz formalism

The pair wave function in Eq. (1), $\Psi(\vec{k}^*, \vec{r}^*)$, depends on the two-particle interaction. Kaons interact with protons via the strong and, for charged kaons, also the Coulomb force. In such a scenario, the interaction of two non-identical particles is given by

the Bethe–Salpeter amplitude, corresponding to the solution of the quantum scattering problem taken in the inverse time direction[3]:

$$\Psi^{(+)}_{-\vec{k}^*}(\vec{r^*}) = \sqrt{A_C(\varepsilon)}\frac{1}{\sqrt{2}}\Big[e^{-i\vec{k}^*\times\vec{r}^*}F(-i\varepsilon, 1, i\zeta^+) + f_C(\vec{k}^*)\frac{\tilde{G}(\rho,\varepsilon)}{r^*}\Big], \quad (A.1)$$

where A_C is the Gamow factor, $\zeta^{\pm} = k^*r^*(1\pm\cos\theta^*)$, $\varepsilon = 1/(k^*a_C)$, F is the confluent hypergeometric function, and $\tilde{G}$ is the combination of the regular and singular s-wave Coulomb functions. The angle θ^* is defined between the pair relative momentum and relative position in the pair rest frame, while a_C is the Bohr radius of the pair ($a_C = -83.59$ fm for K^-p pairs). The component $f_C(k^*)$ is the strong-interaction scattering amplitude, modified by the Coulomb component:

$$f_C^{-1}(k^*) = \frac{1}{f_0} + \frac{1}{2}d_0k^{*2} - \frac{2}{a_C}h(k^*a_C) - ik^*a_C, \quad (A.2)$$

where $h(\varepsilon) = \varepsilon^2\sum_{n=1}^{\infty}[n(n^2+\varepsilon^2)]^{-1} - \gamma - \ln|\varepsilon|$ ($\gamma = 0.5772$ is the Euler constant).

Moreover, the description becomes more complicated when coupled channels are present. For details, see Refs. [51,81].

The correlation function is obtained by numerical integration of the source function $S(r^*)$, parameterised by a three-dimensional Gaussian in the PRF, with the Bethe–Salpeter amplitude given in Eq. (A.1) and with the Coulomb-modified scattering amplitude defined in Eq. (A.2) [74,82].

References

[1] A.A. Petrov, A.E. Blechman, Effective Field Theories, World Scientific, 2016.
[2] E. Leader, Spin in Particle Physics, vol. 5, 2011, p. 2.
[3] H. Wiedemann, Particle Accelerator Physics, 4th ed., Springer, Berlin, 2015.
[4] W.E. Humphrey, R.R. Ross, Low-energy interactions of K^- mesons in hydrogen, Phys. Rev. 127 (1962) 1305–1323.
[5] M. Sakitt, T. Day, R. Glasser, N. Seeman, J. Friedman, W. Humphrey, R. Ross, Low-energy K^- meson interactions in hydrogen, Phys. Rev. 139 (1965) B719.
[6] J. Kim, Low energy K^-−p interaction and interpretation of the 1405-MeV Y_0^* resonance as a $\bar{K}N$ bound state, Phys. Rev. Lett. 14 (1965) 29.
[7] J. Kim, Multichannel phase-shift analysis of $\bar{K}N$ interaction in the region 0 to 550 MeV/c, Phys. Rev. Lett. 19 (1967) 1074.
[8] W. Kittel, G. Otter, I. Wacek, The K^-p charge exchange interactions at low energies and scattering lengths determination, Phys. Lett. 21 (1966) 349–351.
[9] D. Evans, J. Major, E. Rondio, J.A. Zakrzewski, J. Conboy, D. Miller, T. Tymieniecka, Charge exchange scattering in K^-p interactions below 300 MeV/c, J. Phys. G 9 (1983) 885–894.
[10] J. Ciborowski, et al., Kaon scattering and charged sigma hyperon production in K^-p interactions below 300 MeV/c, J. Phys. G 8 (1982) 13–32.
[11] J. Gasser, V. Lyubovitskij, A. Rusetsky, Hadronic atoms, Annu. Rev. Nucl. Part. Sci. 59 (2009) 169–190, arXiv:0903.0257 [hep-ph].
[12] C. Curceanu, et al., The modern era of light kaonic atom experiments, Rev. Mod. Phys. 91 (2) (2019) 025006.
[13] C. Batty, E. Friedman, A. Gal, Strong interaction physics from hadronic atoms, Phys. Rep. 287 (5) (1997) 385–445, https://www.sciencedirect.com/science/article/pii/S0370157397000112.
[14] M. Hori, H. Aghai-Khozani, A. Sótér, A. Dax, D. Barna, Laser spectroscopy of pionic helium atoms, Nature 581 (7806) (2020) 37–41.
[15] S. Deser, M. Goldberger, K. Baumann, W.E. Thirring, Energy level displacements in pi mesonic atoms, Phys. Rev. 96 (1954) 774–776.
[16] U.G. Meissner, U. Raha, A. Rusetsky, Spectrum and decays of kaonic hydrogen, Eur. Phys. J. C 35 (2004) 349–357, arXiv:hep-ph/0402261.
[17] Y. Ikeda, T. Hyodo, W. Weise, Improved constraints on chiral SU(3) dynamics from kaonic hydrogen, Phys. Lett. B 706 (2011) 63–67, arXiv:1109.3005 [nucl-th].
[18] Y. Ikeda, T. Hyodo, W. Weise, Chiral SU(3) theory of antikaon-nucleon interactions with improved threshold constraints, Nucl. Phys. A 881 (2012) 98–114, arXiv:1201.6549 [nucl-th].
[19] SIDDHARTA Collaboration, M. Bazzi, et al., A new measurement of kaonic hydrogen X-rays, Phys. Lett. B 704 (2011) 113–117, arXiv:1105.3090 [nucl-ex].
[20] M. Bazzi, et al., Kaonic hydrogen X-ray measurement in SIDDHARTA, Nucl. Phys. A 881 (2012) 88–97, arXiv:1201.4635 [nucl-ex].
[21] SIDDHARTA Collaboration, J. Zmeskal, et al., Kaonic atoms at DAFNE: the SIDDHARTA experiment, Int. J. Mod. Phys. A 24 (2009) 190–197.
[22] A. Ghigo, G. Mazzitelli, F. Sannibale, P. Valente, G. Vignola, Commissioning of the DAFNE beam test facility, Nucl. Instrum. Methods A 515 (2003) 524–542.
[23] T. Hyodo, D. Jido, The nature of the lambda(1405) resonance in chiral dynamics, Prog. Part. Nucl. Phys. 67 (2012) 55–98, arXiv:1104.4474 [nucl-th].
[24] D. Gotta, Precision spectroscopy of light exotic atoms, Prog. Part. Nucl. Phys. 52 (2004) 133–195.
[25] E. Klempt, F. Bradamante, A. Martin, J. Richard, Antinucleon nucleon interaction at low energy: scattering and protonium, Phys. Rep. 368 (2002) 119–316.
[26] R. Dalitz, S. Tuan, The phenomenological description of -k-nucleon reaction processes, Ann. Phys. 10 (1960) 307–351.
[27] D. Hadjimichef, J. Haidenbauer, G. Krein, Short range repulsion and isospin dependence in the KN system, Phys. Rev. C 66 (2002) 055214, arXiv:nucl-th/0209026.
[28] W.R. Gibbs, R. Arceo, Partial-wave analysis of K^+ nucleon scattering, Phys. Rev. C 75 (2007) 035204, arXiv:nucl-th/0611095 [nucl-th].
[29] ALICE Collaboration, J. Adam, et al., Enhanced production of multi-strange hadrons in high-multiplicity proton-proton collisions, Nat. Phys. 13 (2017) 535–539, arXiv:1606.07424 [nucl-ex].
[30] ALICE Collaboration, B. Abelev, et al., K^0_S and Λ production in Pb-Pb collisions at $\sqrt{s_{NN}} = 2.76$ TeV, Phys. Rev. Lett. 111 (2013) 222301, arXiv:1307.5530 [nucl-ex].
[31] ALICE Collaboration, B. Abelev, et al., Pion, kaon, and proton production in central Pb–Pb collisions at $\sqrt{s_{NN}} = 2.76$ TeV, Phys. Rev. Lett. 109 (2012) 252301, arXiv:1208.1974 [hep-ex].
[32] ALICE Collaboration, B. Abelev, et al., Centrality dependence of π, k, p production in Pb-Pb collisions at $\sqrt{s_{NN}} = 2.76$ TeV, Phys. Rev. C 88 (2013) 044910, arXiv:1303.0737 [hep-ex].
[33] A. Andronic, P. Braun-Munzinger, K. Redlich, J. Stachel, Decoding the phase structure of QCD via particle production at high energy, Nature 561 (7723) (2018) 321–330, arXiv:1710.09425 [nucl-th].
[34] STAR Collaboration, L. Adamczyk, et al., Measurement of interaction between antiprotons, Nature 527 (2015) 345–348, arXiv:1507.07158 [nucl-ex].
[35] STAR Collaboration, J. Adam, et al., The proton-Ω correlation function in Au+Au collisions at $\sqrt{s_{NN}} = 200$ GeV, Phys. Lett. B 790 (2019) 490–497, arXiv:1808.02511 [hep-ex].
[36] ALICE Collaboration, S. Acharya, et al., Measurement of strange baryon–antibaryon interactions with femtoscopic correlations, Phys. Lett. B 802 (2020) 135223, arXiv:1903.06149 [nucl-ex].
[37] ALICE Collaboration, S. Acharya, et al., Scattering studies with low-energy kaon-proton femtoscopy in proton-proton collisions at the LHC, Phys. Rev. Lett. 124 (9) (2020) 092301, arXiv:1905.13470 [nucl-ex].
[38] ALICE Collaboration, K. Aamodt, et al., The ALICE experiment at the CERN LHC, J. Instrum. 3 (2008) S08002.
[39] Y. Kamiya, T. Hyodo, K. Morita, A. Ohnishi, W. Weise, K^-p correlation function from high-energy nuclear collisions and chiral SU(3) dynamics, Phys. Rev. Lett. 124 (13) (2020) 132501, arXiv:1911.01041 [nucl-th].
[40] R. Lednický, V.L. Lyuboshitz, Final state interaction effect on pairing correlations between particles with small relative momenta, Sov. J. Nucl. Phys. 35 (1982) 770, Yad. Fiz. 35 (1981) 1316.
[41] R. Lednický, Correlation femtoscopy of multiparticle processes, Phys. At. Nucl. 67 (2004) 72–82, arXiv:nucl-th/0305027 [nucl-th], Yad. Fiz. 67 (2004) 73.
[42] L. Evans, P. Bryant, LHC machine, J. Instrum. 3 (2008) S08001.
[43] ALICE Collaboration, B. Abelev, et al., Performance of the ALICE experiment at the CERN LHC, Int. J. Mod. Phys. A 29 (2014) 1430044, arXiv:1402.4476 [nucl-ex].
[44] ALICE Collaboration, B. Abelev, et al., Centrality determination of Pb–Pb collisions at $\sqrt{s_{NN}} = 2.76$ TeV with ALICE, Phys. Rev. C 88 (4) (2013) 044909, arXiv:1301.4361 [nucl-ex].
[45] ALICE Collaboration, J. Adam, et al., Centrality dependence of the charged-particle multiplicity density at midrapidity in Pb–Pb collisions at $\sqrt{s_{NN}} = 5.02$ TeV, Phys. Rev. Lett. 116 (22) (2016) 222302, arXiv:1512.06104 [nucl-ex].
[46] ALICE Collaboration, G. Dellacasa, et al., ALICE time projection chamber: Technical Design Report, CERN-LHCC-2000–001, http://cds.cern.ch/record/451098, 2000.
[47] A. Akindinov, et al., Performance of the ALICE Time-Of-Flight detector at the LHC, Eur. Phys. J. Plus 128 (2013) 44.
[48] X.-N. Wang, M. Gyulassy, HIJING: a Monte Carlo model for multiple jet production in pp, p A and A A collisions, Phys. Rev. D 44 (1991) 3501–3516.
[49] R. Brun, F. Bruyant, F. Carminati, S. Giani, M. Maire, A. McPherson, G. Patrick, L. Urban, GEANT: Detector Description and Simulation Tool, Oct 1994, Long Writeup W5013, CERN Program Library, CERN, Geneva, 1993, http://cds.cern.ch/record/1082634.
[50] M.A. Lisa, S. Pratt, R. Soltz, U. Wiedemann, Femtoscopy in relativistic heavy ion collisions, Annu. Rev. Nucl. Part. Sci. 55 (2005) 357–402, arXiv:nucl-ex/0505014.

[3] The inverse time direction is manifested by the "−" sign in front of k^*.

[51] R. Lednický, Finite-size effects on two-particle production in continuous and discrete spectrum, Phys. Part. Nucl. 40 (2009) 307–352, arXiv:nucl-th/0501065.
[52] S.E. Koonin, Proton pictures of high-energy nuclear collisions, Phys. Lett. B 70 (1977) 43–47.
[53] S. Pratt, T. Csorgo, J. Zimanyi, Detailed predictions for two-pion correlations in ultrarelativistic heavy-ion collisions, Phys. Rev. C 42 (1990) 2646–2652.
[54] R. Lednický, Femtoscopic correlations of nonidentical particles, Acta Phys. Pol. B 40 (2009) 1145–1154.
[55] G.I. Kopylov, Like particle correlations as a tool to study the multiple production mechanism, Phys. Lett. B 50 (1974) 472–474.
[56] ALICE Collaboration, S. Acharya, et al., Kaon femtoscopy in Pb-Pb collisions at $\sqrt{s_{\rm NN}} = 2.76$ TeV, Phys. Rev. C 96 (6) (2017) 064613, arXiv:1709.01731 [nucl-ex].
[57] ALICE Collaboration, S. Acharya, et al., Unveiling the strong interaction among hadrons at the LHC, Nature 588 (2020) 232–238, arXiv:2005.11495 [nucl-ex].
[58] A. Kisiel, Non-identical particle correlation analysis in the presence of non-femtoscopic correlations, Acta Phys. Pol. B 48 (2017) 717.
[59] P. Bozek, I. Wyskiel-Piekarska, Particle spectra in Pb-Pb collisions at $\sqrt{s_{NN}} = 2.76$ TeV, Phys. Rev. C 85 (2012) 064915, arXiv:1203.6513 [nucl-th].
[60] M. Chojnacki, A. Kisiel, W. Florkowski, W. Broniowski, THERMINATOR 2: THERMal heavy IoN generATOR 2, Comput. Phys. Commun. 183 (2012) 746–773, arXiv:1102.0273 [nucl-th].
[61] Z.-W. Lin, C.M. Ko, B.-A. Li, B. Zhang, S. Pal, A multi-phase transport model for relativistic heavy ion collisions, Phys. Rev. C 72 (2005) 064901, arXiv:nucl-th/0411110.
[62] W. Broniowski, M. Chojnacki, W. Florkowski, A. Kisiel, Uniform description of soft observables in heavy-ion collisions at $\sqrt{s_{\rm NN}} = 200$ GeV, Phys. Rev. Lett. 101 (2008) 022301, arXiv:0801.4361 [nucl-th].
[63] ALICE Collaboration, S. Acharya, et al., Pion-kaon femtoscopy and the lifetime of the hadronic phase in Pb−Pb collisions at $\sqrt{s_{\rm NN}} = 2.76$ TeV, Phys. Lett. B 813 (2021) 136030, arXiv:2007.08315 [nucl-ex].
[64] P. Huovinen, P. Ruuskanen, Hydrodynamic models for heavy ion collisions, Annu. Rev. Nucl. Part. Sci. 56 (2006) 163–206, arXiv:nucl-th/0605008.
[65] C. Gale, S. Jeon, B. Schenke, Hydrodynamic modeling of heavy-ion collisions, Int. J. Mod. Phys. A 28 (2013) 1340011, arXiv:1301.5893 [nucl-th].
[66] P. Foka, M.A. Janik, An overview of experimental results from ultra-relativistic heavy-ion collisions at the CERN LHC: bulk properties and dynamical evolution, Rev. Phys. 1 (2016) 154–171, arXiv:1702.07233 [hep-ex].
[67] ALICE Collaboration, J. Adam, et al., Anisotropic flow of charged particles in Pb-Pb collisions at $\sqrt{s_{\rm NN}} = 5.02$ TeV, Phys. Rev. Lett. 116 (13) (2016) 132302, arXiv:1602.01119 [nucl-ex].
[68] ALICE Collaboration, B. Abelev, et al., Production of charged pions, kaons and protons at large transverse momenta in pp and Pb–Pb collisions at $\sqrt{s_{\rm NN}} = 2.76$ TeV, Phys. Lett. B 736 (2014) 196–207, arXiv:1401.1250 [nucl-ex].
[69] ALICE Collaboration, J. Adam, et al., One-dimensional pion, kaon, and proton femtoscopy in Pb-Pb collisions at $\sqrt{s_{\rm NN}} = 2.76$ TeV, Phys. Rev. C 92 (5) (2015) 054908, arXiv:1506.07884 [nucl-ex].
[70] CERES Collaboration, D. Adamová, et al., Beam energy and centrality dependence of two pion Bose-Einstein correlations at SPS energies, Nucl. Phys. A 714 (2003) 124–144, arXiv:nucl-ex/0207005.
[71] STAR Collaboration, J. Adams, et al., Pion interferometry in Au+Au collisions at $\sqrt{s_{\rm NN}} = 200$ GeV, Phys. Rev. C 71 (2005) 044906, arXiv:nucl-ex/0411036.
[72] STAR Collaboration, B.I. Abelev, et al., Pion Interferometry in Au+Au and Cu+Cu Collisions at RHIC, Phys. Rev. C 80 (2009) 024905, arXiv:0903.1296 [nucl-ex].
[73] ALICE Collaboration, J. Adam, et al., Centrality dependence of pion freeze-out radii in Pb–Pb collisions at $\sqrt{s_{\rm NN}} = 2.76$ TeV, Phys. Rev. C 93 (2) (2016) 024905, arXiv:1507.06842 [nucl-ex].
[74] A. Kisiel, Non-identical particle femtoscopy at $\sqrt{s_{\rm NN}} = 200$ GeV in hydrodynamics with statistical hadronization, Phys. Rev. C 81 (2010) 064906, arXiv:0909.5349 [nucl-th].
[75] A.D. Martin, Kaon - nucleon parameters, Nucl. Phys. B 179 (1981) 33–48.
[76] T. Ito, et al., Observation of kaonic hydrogen atom X rays, Phys. Rev. C 58 (1998) 2366–2382.
[77] Z.-W. Liu, J.-J. Wu, D.B. Leinweber, A.W. Thomas, Kaonic hydrogen and deuterium in Hamiltonian effective field theory, Phys. Lett. B 808 (2020) 135652, arXiv:2003.09181.
[78] T. Hoshino, S. Ohnishi, W. Horiuchi, T. Hyodo, W. Weise, Constraining the $\bar{K}N$ interaction from the 1S level shift of kaonic deuterium, Phys. Rev. C 96 (4) (2017) 045204, arXiv:1705.06857 [nucl-th].
[79] B. Borasoy, U.-G. Meissner, R. Nissler, K^-p scattering length from scattering experiments, Phys. Rev. C 74 (2006) 055201, arXiv:hep-ph/0606108.
[80] D. Mihaylov, V. Mantovani Sarti, O. Arnold, L. Fabbietti, B. Hohlweger, A. Mathis, A femtoscopic correlation analysis tool using the Schrödinger equation (CATS), Eur. Phys. J. C 78 (5) (2018) 394, arXiv:1802.08481 [hep-ph].
[81] J. Haidenbauer, Coupled-channel effects in hadron–hadron correlation functions, Nucl. Phys. A 981 (2019) 1–16, arXiv:1808.05049 [hep-ph].
[82] A. Kisiel, Pion-kaon femtoscopy in Pb–Pb collisions at $\sqrt{s_{\rm NN}} = 2.76$ TeV modeled in (3 + 1) D hydrodynamics coupled to Therminator 2 and the effect of delayed kaon emission, Phys. Rev. C 98 (4) (2018) 044909, arXiv:1804.06781 [nucl-th].

ALICE Collaboration

S. Acharya [143], D. Adamová [98], A. Adler [76], J. Adolfsson [83], G. Aglieri Rinella [35], M. Agnello [31], N. Agrawal [55], Z. Ahammed [143], S. Ahmad [16], S.U. Ahn [78], I. Ahuja [39], Z. Akbar [52], A. Akindinov [95], M. Al-Turany [110], S.N. Alam [41], D. Aleksandrov [91], B. Alessandro [61], H.M. Alfanda [7], R. Alfaro Molina [73], B. Ali [16], Y. Ali [14], A. Alici [26], N. Alizadehvandchali [127], A. Alkin [35], J. Alme [21], T. Alt [70], L. Altenkamper [21], I. Altsybeev [115], M.N. Anaam [7], C. Andrei [49], D. Andreou [93], A. Andronic [146], M. Angeletti [35], V. Anguelov [107], F. Antinori [58], P. Antonioli [55], C. Anuj [16], N. Apadula [82], L. Aphecetche [117], H. Appelshäuser [70], S. Arcelli [26], R. Arnaldi [61], I.C. Arsene [20], M. Arslandok [148,107], A. Augustinus [35], R. Averbeck [110], S. Aziz [80], M.D. Azmi [16], A. Badalà [57], Y.W. Baek [42], X. Bai [131,110], R. Bailhache [70], Y. Bailung [51], R. Bala [104], A. Balbino [31], A. Baldisseri [140], B. Balis [2], M. Ball [44], D. Banerjee [4], R. Barbera [27], L. Barioglio [108,25], M. Barlou [87], G.G. Barnaföldi [147], L.S. Barnby [97], V. Barret [137], C. Bartels [130], K. Barth [35], E. Bartsch [70], F. Baruffaldi [28], N. Bastid [137], S. Basu [83], G. Batigne [117], B. Batyunya [77], D. Bauri [50], J.L. Bazo Alba [114], I.G. Bearden [92], C. Beattie [148], I. Belikov [139], A.D.C. Bell Hechavarria [146], F. Bellini [26,35], R. Bellwied [127], S. Belokurova [115], V. Belyaev [96], G. Bencedi [71], S. Beole [25], A. Bercuci [49], Y. Berdnikov [101], A. Berdnikova [107], D. Berenyi [147], L. Bergmann [107], M.G. Besoiu [69], L. Betev [35], P.P. Bhaduri [143], A. Bhasin [104], I.R. Bhat [104], M.A. Bhat [4], B. Bhattacharjee [43], P. Bhattacharya [23], L. Bianchi [25], N. Bianchi [53], J. Bielčík [38], J. Bielčíková [98], J. Biernat [120], A. Bilandzic [108], G. Biro [147], S. Biswas [4], J.T. Blair [121], D. Blau [91], M.B. Blidaru [110], C. Blume [70], G. Boca [29,59], F. Bock [99], A. Bogdanov [96], S. Boi [23], J. Bok [63], L. Boldizsár [147], A. Bolozdynya [96], M. Bombara [39], P.M. Bond [35], G. Bonomi [142,59], H. Borel [140], A. Borissov [84], H. Bossi [148], E. Botta [25], L. Bratrud [70], P. Braun-Munzinger [110], M. Bregant [123], M. Broz [38], G.E. Bruno [109,34], M.D. Buckland [130], D. Budnikov [111], H. Buesching [70], S. Bufalino [31], O. Bugnon [117], P. Buhler [116], Z. Buthelezi [74,134], J.B. Butt [14], S.A. Bysiak [120], D. Caffarri [93], M. Cai [28,7], H. Caines [148], A. Caliva [110], E. Calvo Villar [114], J.M.M. Camacho [122], R.S. Camacho [46], P. Camerini [24], F.D.M. Canedo [123],

F. Carnesecchi [35,26], R. Caron [140], J. Castillo Castellanos [140], E.A.R. Casula [23], F. Catalano [31], C. Ceballos Sanchez [77], P. Chakraborty [50], S. Chandra [143], S. Chapeland [35], M. Chartier [130], S. Chattopadhyay [143], S. Chattopadhyay [112], A. Chauvin [23], T.G. Chavez [46], C. Cheshkov [138], B. Cheynis [138], V. Chibante Barroso [35], D.D. Chinellato [124], S. Cho [63], P. Chochula [35], P. Christakoglou [93], C.H. Christensen [92], P. Christiansen [83], T. Chujo [136], C. Cicalo [56], L. Cifarelli [26], F. Cindolo [55], M.R. Ciupek [110], G. Clai [55,II], J. Cleymans [126,I], F. Colamaria [54], J.S. Colburn [113], D. Colella [109,54,34,147], A. Collu [82], M. Colocci [35,26], M. Concas [61,III], G. Conesa Balbastre [81], Z. Conesa del Valle [80], G. Contin [24], J.G. Contreras [38], M.L. Coquet [140], T.M. Cormier [99], P. Cortese [32], M.R. Cosentino [125], F. Costa [35], S. Costanza [29,59], P. Crochet [137], E. Cuautle [71], P. Cui [7], L. Cunqueiro [99], A. Dainese [58], F.P.A. Damas [117,140], M.C. Danisch [107], A. Danu [69], I. Das [112], P. Das [89], P. Das [4], S. Das [4], S. Dash [50], S. De [89], A. De Caro [30], G. de Cataldo [54], L. De Cilladi [25], J. de Cuveland [40], A. De Falco [23], D. De Gruttola [30], N. De Marco [61], C. De Martin [24], S. De Pasquale [30], S. Deb [51], H.F. Degenhardt [123], K.R. Deja [144], L. Dello Stritto [30], S. Delsanto [25], W. Deng [7], P. Dhankher [19], D. Di Bari [34], A. Di Mauro [35], R.A. Diaz [8], T. Dietel [126], Y. Ding [138,7], R. Divià [35], D.U. Dixit [19], Ø. Djuvsland [21], U. Dmitrieva [65], J. Do [63], A. Dobrin [69], B. Dönigus [70], O. Dordic [20], A.K. Dubey [143], A. Dubla [110,93], S. Dudi [103], M. Dukhishyam [89], P. Dupieux [137], N. Dzalaiova [13], T.M. Eder [146], R.J. Ehlers [99], V.N. Eikeland [21], D. Elia [54], B. Erazmus [117], F. Ercolessi [26], F. Erhardt [102], A. Erokhin [115], M.R. Ersdal [21], B. Espagnon [80], G. Eulisse [35], D. Evans [113], S. Evdokimov [94], L. Fabbietti [108], M. Faggin [28], J. Faivre [81], F. Fan [7], A. Fantoni [53], M. Fasel [99], P. Fecchio [31], A. Feliciello [61], G. Feofilov [115], A. Fernández Téllez [46], A. Ferrero [140], A. Ferretti [25], V.J.G. Feuillard [107], J. Figiel [120], S. Filchagin [111], D. Finogeev [65], F.M. Fionda [56,21], G. Fiorenza [35,109], F. Flor [127], A.N. Flores [121], S. Foertsch [74], P. Foka [110], S. Fokin [91], E. Fragiacomo [62], E. Frajna [147], U. Fuchs [35], N. Funicello [30], C. Furget [81], A. Furs [65], J.J. Gaardhøje [92], M. Gagliardi [25], A.M. Gago [114], A. Gal [139], C.D. Galvan [122], P. Ganoti [87], C. Garabatos [110], J.R.A. Garcia [46], E. Garcia-Solis [10], K. Garg [117], C. Gargiulo [35], A. Garibli [90], K. Garner [146], P. Gasik [110], E.F. Gauger [121], A. Gautam [129], M.B. Gay Ducati [72], M. Germain [117], J. Ghosh [112], P. Ghosh [143], S.K. Ghosh [4], M. Giacalone [26], P. Gianotti [53], P. Giubellino [110,61], P. Giubilato [28], A.M.C. Glaenzer [140], P. Glässel [107], D.J.Q. Goh [85], V. Gonzalez [145], L.H. González-Trueba [73], S. Gorbunov [40], M. Gorgon [2], L. Görlich [120], S. Gotovac [36], V. Grabski [73], L.K. Graczykowski [144], L. Greiner [82], A. Grelli [64], C. Grigoras [35], V. Grigoriev [96], A. Grigoryan [1,I], S. Grigoryan [77,1], O.S. Groettvik [21], F. Grosa [35,61], J.F. Grosse-Oetringhaus [35], R. Grosso [110], G.G. Guardiano [124], R. Guernane [81], M. Guilbaud [117], K. Gulbrandsen [92], T. Gunji [135], A. Gupta [104], R. Gupta [104], I.B. Guzman [46], S.P. Guzman [46], L. Gyulai [147], M.K. Habib [110], C. Hadjidakis [80], G. Halimoglu [70], H. Hamagaki [85], G. Hamar [147], M. Hamid [7], R. Hannigan [121], M.R. Haque [144,89], A. Harlenderova [110], J.W. Harris [148], A. Harton [10], J.A. Hasenbichler [35], H. Hassan [99], D. Hatzifotiadou [55], P. Hauer [44], L.B. Havener [148], S. Hayashi [135], S.T. Heckel [108], E. Hellbär [70], H. Helstrup [37], T. Herman [38], E.G. Hernandez [46], G. Herrera Corral [9], F. Herrmann [146], K.F. Hetland [37], H. Hillemanns [35], C. Hills [130], B. Hippolyte [139], B. Hofman [64], B. Hohlweger [93,108], J. Honermann [146], G.H. Hong [149], D. Horak [38], S. Hornung [110], A. Horzyk [2], R. Hosokawa [15], P. Hristov [35], C. Huang [80], C. Hughes [133], P. Huhn [70], T.J. Humanic [100], H. Hushnud [112], L.A. Husova [146], A. Hutson [127], D. Hutter [40], J.P. Iddon [35,130], R. Ilkaev [111], H. Ilyas [14], M. Inaba [136], G.M. Innocenti [35], M. Ippolitov [91], A. Isakov [38,98], M.S. Islam [112], M. Ivanov [110], V. Ivanov [101], V. Izucheev [94], M. Jablonski [2], B. Jacak [82], N. Jacazio [35], P.M. Jacobs [82], S. Jadlovska [119], J. Jadlovsky [119], S. Jaelani [64], C. Jahnke [124,123], M.J. Jakubowska [144], M.A. Janik [144], T. Janson [76], M. Jercic [102], O. Jevons [113], F. Jonas [99,146], P.G. Jones [113], J.M. Jowett [35,110], J. Jung [70], M. Jung [70], A. Junique [35], A. Jusko [113], J. Kaewjai [118], P. Kalinak [66], A. Kalweit [35], V. Kaplin [96], S. Kar [7], A. Karasu Uysal [79], D. Karatovic [102], O. Karavichev [65], T. Karavicheva [65], P. Karczmarczyk [144], E. Karpechev [65], A. Kazantsev [91], U. Kebschull [76], R. Keidel [48], D.L.D. Keijdener [64], M. Keil [35], B. Ketzer [44], Z. Khabanova [93], A.M. Khan [7], S. Khan [16], A. Khanzadeev [101], Y. Kharlov [94], A. Khatun [16], A. Khuntia [120], B. Kileng [37], B. Kim [17,63], D. Kim [149], D.J. Kim [128], E.J. Kim [75], J. Kim [149], J.S. Kim [42], J. Kim [107], J. Kim [149], J. Kim [75], M. Kim [107], S. Kim [18], T. Kim [149], S. Kirsch [70], I. Kisel [40], S. Kiselev [95], A. Kisiel [144], J.P. Kitowski [2], J.L. Klay [6], J. Klein [35], S. Klein [82], C. Klein-Bösing [146], M. Kleiner [70], T. Klemenz [108], A. Kluge [35], A.G. Knospe [127], C. Kobdaj [118], M.K. Köhler [107], T. Kollegger [110], A. Kondratyev [77], N. Kondratyeva [96], E. Kondratyuk [94], J. Konig [70], S.A. Konigstorfer [108], P.J. Konopka [35,2], G. Kornakov [144], S.D. Koryciak [2], L. Koska [119], A. Kotliarov [98], O. Kovalenko [88], V. Kovalenko [115], M. Kowalski [120], I. Králik [66], A. Kravčáková [39], L. Kreis [110], M. Krivda [113,66], F. Krizek [98], K. Krizkova Gajdosova [38], M. Kroesen [107], M. Krüger [70], E. Kryshen [101], M. Krzewicki [40], V. Kučera [35], C. Kuhn [139], P.G. Kuijer [93], T. Kumaoka [136],

D. Kumar [143], L. Kumar [103], N. Kumar [103], S. Kundu [35,89], P. Kurashvili [88], A. Kurepin [65], A.B. Kurepin [65], A. Kuryakin [111], S. Kushpil [98], J. Kvapil [113], M.J. Kweon [63], J.Y. Kwon [63], Y. Kwon [149], S.L. La Pointe [40], P. La Rocca [27], Y.S. Lai [82], A. Lakrathok [118], M. Lamanna [35], R. Langoy [132], K. Lapidus [35], P. Larionov [53], E. Laudi [35], L. Lautner [35,108], R. Lavicka [38], T. Lazareva [115], R. Lea [142,24,59], J. Lee [136], J. Lehrbach [40], R.C. Lemmon [97], I. León Monzón [122], E.D. Lesser [19], M. Lettrich [35,108], P. Lévai [147], X. Li [11], X.L. Li [7], J. Lien [132], R. Lietava [113], B. Lim [17], S.H. Lim [17], V. Lindenstruth [40], A. Lindner [49], C. Lippmann [110], A. Liu [19], J. Liu [130], I.M. Lofnes [21], V. Loginov [96], C. Loizides [99], P. Loncar [36], J.A. Lopez [107], X. Lopez [137], E. López Torres [8], J.R. Luhder [146], M. Lunardon [28], G. Luparello [62], Y.G. Ma [41], A. Maevskaya [65], M. Mager [35], T. Mahmoud [44], A. Maire [139], M. Malaev [101], Q.W. Malik [20], L. Malinina [77,IV], D. Mal'Kevich [95], N. Mallick [51], P. Malzacher [110], G. Mandaglio [33,57], V. Manko [91], F. Manso [137], V. Manzari [54], Y. Mao [7], J. Mareš [68], G.V. Margagliotti [24], A. Margotti [55], A. Marín [110], C. Markert [121], M. Marquard [70], N.A. Martin [107], P. Martinengo [35], J.L. Martinez [127], M.I. Martínez [46], G. Martínez García [117], S. Masciocchi [110], M. Masera [25], A. Masoni [56], L. Massacrier [80], A. Mastroserio [141,54], A.M. Mathis [108], O. Matonoha [83], P.F.T. Matuoka [123], A. Matyja [120], C. Mayer [120], A.L. Mazuecos [35], F. Mazzaschi [25], M. Mazzilli [35], M.A. Mazzoni [60], J.E. Mdhluli [134], A.F. Mechler [70], F. Meddi [22], Y. Melikyan [65], A. Menchaca-Rocha [73], E. Meninno [116,30], A.S. Menon [127], M. Meres [13], S. Mhlanga [126,74], Y. Miake [136], L. Micheletti [61,25], L.C. Migliorin [138], D.L. Mihaylov [108], K. Mikhaylov [77,95], A.N. Mishra [147], D. Miśkowiec [110], A. Modak [4], A.P. Mohanty [64], B. Mohanty [89], M. Mohisin Khan [16], Z. Moravcova [92], C. Mordasini [108], D.A. Moreira De Godoy [146], L.A.P. Moreno [46], I. Morozov [65], A. Morsch [35], T. Mrnjavac [35], V. Muccifora [53], E. Mudnic [36], D. Mühlheim [146], S. Muhuri [143], J.D. Mulligan [82], A. Mulliri [23], M.G. Munhoz [123], R.H. Munzer [70], H. Murakami [135], S. Murray [126], L. Musa [35], J. Musinsky [66], C.J. Myers [127], J.W. Myrcha [144], B. Naik [134,50], R. Nair [88], B.K. Nandi [50], R. Nania [55], E. Nappi [54], M.U. Naru [14], A.F. Nassirpour [83], A. Nath [107], C. Nattrass [133], A. Neagu [20], L. Nellen [71], S.V. Nesbo [37], G. Neskovic [40], D. Nesterov [115], B.S. Nielsen [92], S. Nikolaev [91], S. Nikulin [91], V. Nikulin [101], F. Noferini [55], S. Noh [12], P. Nomokonov [77], J. Norman [130], N. Novitzky [136], P. Nowakowski [144], A. Nyanin [91], J. Nystrand [21], M. Ogino [85], A. Ohlson [83], V.A. Okorokov [96], J. Oleniacz [144], A.C. Oliveira Da Silva [133], M.H. Oliver [148], A. Onnerstad [128], C. Oppedisano [61], A. Ortiz Velasquez [71], T. Osako [47], A. Oskarsson [83], J. Otwinowski [120], K. Oyama [85], Y. Pachmayer [107], S. Padhan [50], D. Pagano [142,59], G. Paić [71], A. Palasciano [54], J. Pan [145], S. Panebianco [140], P. Pareek [143], J. Park [63], J.E. Parkkila [128], S.P. Pathak [127], R.N. Patra [104,35], B. Paul [23], J. Pazzini [142,59], H. Pei [7], T. Peitzmann [64], X. Peng [7], L.G. Pereira [72], H. Pereira Da Costa [140], D. Peresunko [91], G.M. Perez [8], S. Perrin [140], Y. Pestov [5], V. Petráček [38], M. Petrovici [49], R.P. Pezzi [72], S. Piano [62], M. Pikna [13], P. Pillot [117], O. Pinazza [55,35], L. Pinsky [127], C. Pinto [27], S. Pisano [53], M. Płoskoń [82], M. Planinic [102], F. Pliquett [70], M.G. Poghosyan [99], B. Polichtchouk [94], S. Politano [31], N. Poljak [102], A. Pop [49], S. Porteboeuf-Houssais [137], J. Porter [82], V. Pozdniakov [77], S.K. Prasad [4], R. Preghenella [55], F. Prino [61], C.A. Pruneau [145], I. Pshenichnov [65], M. Puccio [35], S. Qiu [93], L. Quaglia [25], R.E. Quishpe [127], S. Ragoni [113], A. Rakotozafindrabe [140], L. Ramello [32], F. Rami [139], S.A.R. Ramirez [46], A.G.T. Ramos [34], T.A. Rancien [81], R. Raniwala [105], S. Raniwala [105], S.S. Räsänen [45], R. Rath [51], I. Ravasenga [93], K.F. Read [99,133], A.R. Redelbach [40], K. Redlich [88,V], A. Rehman [21], P. Reichelt [70], F. Reidt [35], H.A. Reme-ness [37], R. Renfordt [70], Z. Rescakova [39], K. Reygers [107], A. Riabov [101], V. Riabov [101], T. Richert [83,92], M. Richter [20], W. Riegler [35], F. Riggi [27], C. Ristea [69], S.P. Rode [51], M. Rodríguez Cahuantzi [46], K. Røed [20], R. Rogalev [94], E. Rogochaya [77], T.S. Rogoschinski [70], D. Rohr [35], D. Röhrich [21], P.F. Rojas [46], P.S. Rokita [144], F. Ronchetti [53], A. Rosano [33,57], E.D. Rosas [71], A. Rossi [58], A. Rotondi [29,59], A. Roy [51], P. Roy [112], S. Roy [50], N. Rubini [26], O.V. Rueda [83], R. Rui [24], B. Rumyantsev [77], P.G. Russek [2], A. Rustamov [90], E. Ryabinkin [91], Y. Ryabov [101], A. Rybicki [120], H. Rytkonen [128], W. Rzesa [144], O.A.M. Saarimaki [45], R. Sadek [117], S. Sadovsky [94], J. Saetre [21], K. Šafařík [38], S.K. Saha [143], S. Saha [89], B. Sahoo [50], P. Sahoo [50], R. Sahoo [51], S. Sahoo [67], D. Sahu [51], P.K. Sahu [67], J. Saini [143], S. Sakai [136], S. Sambyal [104], V. Samsonov [101,96,I], D. Sarkar [145], N. Sarkar [143], P. Sarma [43], V.M. Sarti [108], M.H.P. Sas [148], J. Schambach [99,121], H.S. Scheid [70], C. Schiaua [49], R. Schicker [107], A. Schmah [107], C. Schmidt [110], H.R. Schmidt [106], M.O. Schmidt [107], M. Schmidt [106], N.V. Schmidt [99,70], A.R. Schmier [133], R. Schotter [139], J. Schukraft [35], Y. Schutz [139], K. Schwarz [110], K. Schweda [110], G. Scioli [26], E. Scomparin [61], J.E. Seger [15], Y. Sekiguchi [135], D. Sekihata [135], I. Selyuzhenkov [110,96], S. Senyukov [139], J.J. Seo [63], D. Serebryakov [65], L. Šerkšnytė [108], A. Sevcenco [69], T.J. Shaba [74], A. Shabanov [65], A. Shabetai [117], R. Shahoyan [35], W. Shaikh [112], A. Shangaraev [94], A. Sharma [103], H. Sharma [120], M. Sharma [104], N. Sharma [103], S. Sharma [104], O. Sheibani [127], K. Shigaki [47], M. Shimomura [86], S. Shirinkin [95], Q. Shou [41],

Y. Sibiriak [91], S. Siddhanta [56], T. Siemiarczuk [88], T.F. Silva [123], D. Silvermyr [83], G. Simonetti [35], B. Singh [108], R. Singh [89], R. Singh [104], R. Singh [51], V.K. Singh [143], V. Singhal [143], T. Sinha [112], B. Sitar [13], M. Sitta [32], T.B. Skaali [20], G. Skorodumovs [107], M. Slupecki [45], N. Smirnov [148], R.J.M. Snellings [64], C. Soncco [114], J. Song [127], A. Songmoolnak [118], F. Soramel [28], S. Sorensen [133], I. Sputowska [120], J. Stachel [107], I. Stan [69], P.J. Steffanic [133], S.F. Stiefelmaier [107], D. Stocco [117], I. Storehaug [20], M.M. Storetvedt [37], C.P. Stylianidis [93], A.A.P. Suaide [123], T. Sugitate [47], C. Suire [80], M. Suljic [35], R. Sultanov [95], M. Šumbera [98], V. Sumberia [104], S. Sumowidagdo [52], S. Swain [67], A. Szabo [13], I. Szarka [13], U. Tabassam [14], S.F. Taghavi [108], G. Taillepied [137], J. Takahashi [124], G.J. Tambave [21], S. Tang [137,7], Z. Tang [131], M. Tarhini [117], M.G. Tarzila [49], A. Tauro [35], G. Tejeda Muñoz [46], A. Telesca [35], L. Terlizzi [25], C. Terrevoli [127], G. Tersimonov [3], S. Thakur [143], D. Thomas [121], R. Tieulent [138], A. Tikhonov [65], A.R. Timmins [127], M. Tkacik [119], A. Toia [70], N. Topilskaya [65], M. Toppi [53], F. Torales-Acosta [19], T. Tork [80], R.C. Torres [82], S.R. Torres [38], A. Trifiró [33,57], S. Tripathy [55,71], T. Tripathy [50], S. Trogolo [35,28], G. Trombetta [34], V. Trubnikov [3], W.H. Trzaska [128], T.P. Trzcinski [144], B.A. Trzeciak [38], A. Tumkin [111], R. Turrisi [58], T.S. Tveter [20], K. Ullaland [21], A. Uras [138], M. Urioni [59,142], G.L. Usai [23], M. Vala [39], N. Valle [59,29], S. Vallero [61], N. van der Kolk [64], L.V.R. van Doremalen [64], M. van Leeuwen [93], P. Vande Vyvre [35], D. Varga [147], Z. Varga [147], M. Varga-Kofarago [147], A. Vargas [46], M. Vasileiou [87], A. Vasiliev [91], O. Vázquez Doce [108], V. Vechernin [115], E. Vercellin [25], S. Vergara Limón [46], L. Vermunt [64], R. Vértesi [147], M. Verweij [64], L. Vickovic [36], Z. Vilakazi [134], O. Villalobos Baillie [113], G. Vino [54], A. Vinogradov [91], T. Virgili [30], V. Vislavicius [92], A. Vodopyanov [77], B. Volkel [35], M.A. Völkl [107], K. Voloshin [95], S.A. Voloshin [145], G. Volpe [34], B. von Haller [35], I. Vorobyev [108], D. Voscek [119], N. Vozniuk [65], J. Vrláková [39], B. Wagner [21], C. Wang [41], D. Wang [41], M. Weber [116], R.J.G.V. Weelden [93], A. Wegrzynek [35], S.C. Wenzel [35], J.P. Wessels [146], J. Wiechula [70], J. Wikne [20], G. Wilk [88], J. Wilkinson [110], G.A. Willems [146], B. Windelband [107], M. Winn [140], W.E. Witt [133], J.R. Wright [121], W. Wu [41], Y. Wu [131], R. Xu [7], S. Yalcin [79], Y. Yamaguchi [47], K. Yamakawa [47], S. Yang [21], S. Yano [47,140], Z. Yin [7], H. Yokoyama [64], I.-K. Yoo [17], J.H. Yoon [63], S. Yuan [21], A. Yuncu [107], V. Zaccolo [24], A. Zaman [14], C. Zampolli [35], H.J.C. Zanoli [64], N. Zardoshti [35], A. Zarochentsev [115], P. Závada [68], N. Zaviyalov [111], H. Zbroszczyk [144], M. Zhalov [101], S. Zhang [41], X. Zhang [7], Y. Zhang [131], V. Zherebchevskii [115], Y. Zhi [11], D. Zhou [7], Y. Zhou [92], J. Zhu [7,110], Y. Zhu [7], A. Zichichi [26], G. Zinovjev [3], N. Zurlo [142,59]

[1] *A.I. Alikhanyan National Science Laboratory (Yerevan Physics Institute) Foundation, Yerevan, Armenia*
[2] *AGH University of Science and Technology, Cracow, Poland*
[3] *Bogolyubov Institute for Theoretical Physics, National Academy of Sciences of Ukraine, Kiev, Ukraine*
[4] *Bose Institute, Department of Physics and Centre for Astroparticle Physics and Space Science (CAPSS), Kolkata, India*
[5] *Budker Institute for Nuclear Physics, Novosibirsk, Russia*
[6] *California Polytechnic State University, San Luis Obispo, CA, United States*
[7] *Central China Normal University, Wuhan, China*
[8] *Centro de Aplicaciones Tecnológicas y Desarrollo Nuclear (CEADEN), Havana, Cuba*
[9] *Centro de Investigación y de Estudios Avanzados (CINVESTAV), Mexico City and Mérida, Mexico*
[10] *Chicago State University, Chicago, IL, United States*
[11] *China Institute of Atomic Energy, Beijing, China*
[12] *Chungbuk National University, Cheongju, Republic of Korea*
[13] *Comenius University Bratislava, Faculty of Mathematics, Physics and Informatics, Bratislava, Slovakia*
[14] *COMSATS University Islamabad, Islamabad, Pakistan*
[15] *Creighton University, Omaha, NE, United States*
[16] *Department of Physics, Aligarh Muslim University, Aligarh, India*
[17] *Department of Physics, Pusan National University, Pusan, Republic of Korea*
[18] *Department of Physics, Sejong University, Seoul, Republic of Korea*
[19] *Department of Physics, University of California, Berkeley, CA, United States*
[20] *Department of Physics, University of Oslo, Oslo, Norway*
[21] *Department of Physics and Technology, University of Bergen, Bergen, Norway*
[22] *Dipartimento di Fisica dell'Università 'La Sapienza' and Sezione INFN, Rome, Italy*
[23] *Dipartimento di Fisica dell'Università and Sezione INFN, Cagliari, Italy*
[24] *Dipartimento di Fisica dell'Università and Sezione INFN, Trieste, Italy*
[25] *Dipartimento di Fisica dell'Università and Sezione INFN, Turin, Italy*
[26] *Dipartimento di Fisica e Astronomia dell'Università and Sezione INFN, Bologna, Italy*
[27] *Dipartimento di Fisica e Astronomia dell'Università and Sezione INFN, Catania, Italy*
[28] *Dipartimento di Fisica e Astronomia dell'Università and Sezione INFN, Padova, Italy*
[29] *Dipartimento di Fisica e Nucleare e Teorica, Università di Pavia, Pavia, Italy*
[30] *Dipartimento di Fisica 'E.R. Caianiello' dell'Università and Gruppo Collegato INFN, Salerno, Italy*
[31] *Dipartimento DISAT del Politecnico and Sezione INFN, Turin, Italy*
[32] *Dipartimento di Scienze e Innovazione Tecnologica dell'Università del Piemonte Orientale and INFN Sezione di Torino, Alessandria, Italy*
[33] *Dipartimento di Scienze MIFT, Università di Messina, Messina, Italy*
[34] *Dipartimento Interateneo di Fisica 'M. Merlin' and Sezione INFN, Bari, Italy*
[35] *European Organization for Nuclear Research (CERN), Geneva, Switzerland*
[36] *Faculty of Electrical Engineering, Mechanical Engineering and Naval Architecture, University of Split, Split, Croatia*
[37] *Faculty of Engineering and Science, Western Norway University of Applied Sciences, Bergen, Norway*
[38] *Faculty of Nuclear Sciences and Physical Engineering, Czech Technical University in Prague, Prague, Czech Republic*
[39] *Faculty of Science, P.J. Šafárik University, Košice, Slovakia*

[40] Frankfurt Institute for Advanced Studies, Johann Wolfgang Goethe-Universität Frankfurt, Frankfurt, Germany
[41] Fudan University, Shanghai, China
[42] Gangneung-Wonju National University, Gangneung, Republic of Korea
[43] Gauhati University, Department of Physics, Guwahati, India
[44] Helmholtz-Institut für Strahlen- und Kernphysik, Rheinische Friedrich-Wilhelms-Universität Bonn, Bonn, Germany
[45] Helsinki Institute of Physics (HIP), Helsinki, Finland
[46] High Energy Physics Group, Universidad Autónoma de Puebla, Puebla, Mexico
[47] Hiroshima University, Hiroshima, Japan
[48] Hochschule Worms, Zentrum für Technologietransfer und Telekommunikation (ZTT), Worms, Germany
[49] Horia Hulubei National Institute of Physics and Nuclear Engineering, Bucharest, Romania
[50] Indian Institute of Technology Bombay (IIT), Mumbai, India
[51] Indian Institute of Technology Indore, Indore, India
[52] Indonesian Institute of Sciences, Jakarta, Indonesia
[53] INFN, Laboratori Nazionali di Frascati, Frascati, Italy
[54] INFN, Sezione di Bari, Bari, Italy
[55] INFN, Sezione di Bologna, Bologna, Italy
[56] INFN, Sezione di Cagliari, Cagliari, Italy
[57] INFN, Sezione di Catania, Catania, Italy
[58] INFN, Sezione di Padova, Padova, Italy
[59] INFN, Sezione di Pavia, Pavia, Italy
[60] INFN, Sezione di Roma, Rome, Italy
[61] INFN, Sezione di Torino, Turin, Italy
[62] INFN, Sezione di Trieste, Trieste, Italy
[63] Inha University, Incheon, Republic of Korea
[64] Institute for Gravitational and Subatomic Physics (GRASP), Utrecht University/Nikhef, Utrecht, Netherlands
[65] Institute for Nuclear Research, Academy of Sciences, Moscow, Russia
[66] Institute of Experimental Physics, Slovak Academy of Sciences, Košice, Slovakia
[67] Institute of Physics, Homi Bhabha National Institute, Bhubaneswar, India
[68] Institute of Physics of the Czech Academy of Sciences, Prague, Czech Republic
[69] Institute of Space Science (ISS), Bucharest, Romania
[70] Institut für Kernphysik, Johann Wolfgang Goethe-Universität Frankfurt, Frankfurt, Germany
[71] Instituto de Ciencias Nucleares, Universidad Nacional Autónoma de México, Mexico City, Mexico
[72] Instituto de Física, Universidade Federal do Rio Grande do Sul (UFRGS), Porto Alegre, Brazil
[73] Instituto de Física, Universidad Nacional Autónoma de México, Mexico City, Mexico
[74] iThemba LABS, National Research Foundation, Somerset West, South Africa
[75] Jeonbuk National University, Jeonju, Republic of Korea
[76] Johann-Wolfgang-Goethe Universität Frankfurt Institut für Informatik, Fachbereich Informatik und Mathematik, Frankfurt, Germany
[77] Joint Institute for Nuclear Research (JINR), Dubna, Russia
[78] Korea Institute of Science and Technology Information, Daejeon, Republic of Korea
[79] KTO Karatay University, Konya, Turkey
[80] Laboratoire de Physique des 2 Infinis, Irène Joliot-Curie, Orsay, France
[81] Laboratoire de Physique Subatomique et de Cosmologie, Université Grenoble-Alpes, CNRS-IN2P3, Grenoble, France
[82] Lawrence Berkeley National Laboratory, Berkeley, CA, United States
[83] Lund University Department of Physics, Division of Particle Physics, Lund, Sweden
[84] Moscow Institute for Physics and Technology, Moscow, Russia
[85] Nagasaki Institute of Applied Science, Nagasaki, Japan
[86] Nara Women's University (NWU), Nara, Japan
[87] National and Kapodistrian University of Athens, School of Science, Department of Physics, Athens, Greece
[88] National Centre for Nuclear Research, Warsaw, Poland
[89] National Institute of Science Education and Research, Homi Bhabha National Institute, Jatni, India
[90] National Nuclear Research Center, Baku, Azerbaijan
[91] National Research Centre Kurchatov Institute, Moscow, Russia
[92] Niels Bohr Institute, University of Copenhagen, Copenhagen, Denmark
[93] Nikhef, National institute for subatomic physics, Amsterdam, Netherlands
[94] NRC Kurchatov Institute IHEP, Protvino, Russia
[95] NRC «Kurchatov» Institute - ITEP, Moscow, Russia
[96] NRNU Moscow Engineering Physics Institute, Moscow, Russia
[97] Nuclear Physics Group, STFC Daresbury Laboratory, Daresbury, United Kingdom
[98] Nuclear Physics Institute of the Czech Academy of Sciences, Řež u Prahy, Czech Republic
[99] Oak Ridge National Laboratory, Oak Ridge, TN, United States
[100] Ohio State University, Columbus, OH, United States
[101] Petersburg Nuclear Physics Institute, Gatchina, Russia
[102] Physics department, Faculty of science, University of Zagreb, Zagreb, Croatia
[103] Physics Department, Panjab University, Chandigarh, India
[104] Physics Department, University of Jammu, Jammu, India
[105] Physics Department, University of Rajasthan, Jaipur, India
[106] Physikalisches Institut, Eberhard-Karls-Universität Tübingen, Tübingen, Germany
[107] Physikalisches Institut, Ruprecht-Karls-Universität Heidelberg, Heidelberg, Germany
[108] Physik Department, Technische Universität München, Munich, Germany
[109] Politecnico di Bari and Sezione INFN, Bari, Italy
[110] Research Division and ExtreMe Matter Institute EMMI, GSI Helmholtzzentrum für Schwerionenforschung GmbH, Darmstadt, Germany
[111] Russian Federal Nuclear Center (VNIIEF), Sarov, Russia
[112] Saha Institute of Nuclear Physics, Homi Bhabha National Institute, Kolkata, India
[113] School of Physics and Astronomy, University of Birmingham, Birmingham, United Kingdom
[114] Sección Física, Departamento de Ciencias, Pontificia Universidad Católica del Perú, Lima, Peru
[115] St. Petersburg State University, St. Petersburg, Russia
[116] Stefan Meyer Institut für Subatomare Physik (SMI), Vienna, Austria
[117] SUBATECH, IMT Atlantique, Université de Nantes, CNRS-IN2P3, Nantes, France
[118] Suranaree University of Technology, Nakhon Ratchasima, Thailand
[119] Technical University of Košice, Košice, Slovakia

[120] The Henryk Niewodniczanski Institute of Nuclear Physics, Polish Academy of Sciences, Cracow, Poland
[121] The University of Texas at Austin, Austin, TX, United States
[122] Universidad Autónoma de Sinaloa, Culiacán, Mexico
[123] Universidade de São Paulo (USP), São Paulo, Brazil
[124] Universidade Estadual de Campinas (UNICAMP), Campinas, Brazil
[125] Universidade Federal do ABC, Santo Andre, Brazil
[126] University of Cape Town, Cape Town, South Africa
[127] University of Houston, Houston, TX, United States
[128] University of Jyväskylä, Jyväskylä, Finland
[129] University of Kansas, Lawrence, KS, United States
[130] University of Liverpool, Liverpool, United Kingdom
[131] University of Science and Technology of China, Hefei, China
[132] University of South-Eastern Norway, Tonsberg, Norway
[133] University of Tennessee, Knoxville, TN, United States
[134] University of the Witwatersrand, Johannesburg, South Africa
[135] University of Tokyo, Tokyo, Japan
[136] University of Tsukuba, Tsukuba, Japan
[137] Université Clermont Auvergne, CNRS/IN2P3, LPC, Clermont-Ferrand, France
[138] Université de Lyon, CNRS/IN2P3, Institut de Physique des 2 Infinis de Lyon, Lyon, France
[139] Université de Strasbourg, CNRS, IPHC UMR 7178, F-67000, Strasbourg, France
[140] Université Paris-Saclay Centre d'Etudes de Saclay (CEA), IRFU, Département de Physique Nucléaire (DPhN), Saclay, France
[141] Università degli Studi di Foggia, Foggia, Italy
[142] Università di Brescia, Brescia, Italy
[143] Variable Energy Cyclotron Centre, Homi Bhabha National Institute, Kolkata, India
[144] Warsaw University of Technology, Warsaw, Poland
[145] Wayne State University, Detroit, MI, United States
[146] Westfälische Wilhelms-Universität Münster, Institut für Kernphysik, Münster, Germany
[147] Wigner Research Centre for Physics, Budapest, Hungary
[148] Yale University, New Haven, CT, United States
[149] Yonsei University, Seoul, Republic of Korea

[I] Deceased.
[II] Also at: Italian National Agency for New Technologies, Energy and Sustainable Economic Development (ENEA), Bologna, Italy.
[III] Also at: Dipartimento DET del Politecnico di Torino, Turin, Italy.
[IV] Also at: M.V. Lomonosov Moscow State University, D.V. Skobeltsyn Institute of Nuclear, Physics, Moscow, Russia.
[V] Also at: Institute of Theoretical Physics, University of Wroclaw, Poland.